International Journal of Earth Sciences (2023) 112:297–320
https://doi.org/10.1007/s00531-022-02246-6

ORIGINAL PAPER

Metavolcanic formations in the Paraautochthonous Triassic successions of the Bükk Mts, NE Hungary

Norbert Németh[1] · **Ferenc Kristály**[1] · **Péter Gál**[2,5] · **Ferenc Móricz**[1] · **Réka Lukács**[3,4,5]

Received: 26 July 2021 / Accepted: 17 August 2022 / Published online: 4 September 2022

Abstract

The Bükk Mts. in NE Hungary exposes Paleozoic and Mesozoic successions containing volcanic formations both in the oceanic crust-derived Szarvaskő Unit and in the continental crust-derived Paraautochthonous Unit. The rocks of this latter unit were subject of multiple metamorphic, also metasomatic alterations and deformation events obscuring and overprinting original petrographic and geochemical characteristics and producing a complex structure in which stratigraphic relationships are not always possible to be identified. This situation was leading to various stratigraphic hypotheses. This study aims to provide a basis for distinguishing metavolcanic formations using trace element geochemical data combined with quantitative mineralogical data based on XRD and EPMA. Our data were obtained from a wide range of samples collected in the Bükk Mts. Mineralogy and major element geochemistry reflect regional Alpine metamorphism and local alteration processes but high field strength elements remained relatively stable during most of these processes except local HFSE enrichment. Zr/TiO_2, Nb/Y and Nb/Ta ratios were effectively used for classifying the rocks into three formations: Bagolyhegy Metarhyolite, Szentistvánhegy Metavolcanics and Szinva Metabasalt. Bagolyhegy Metarhyolite is a unique volcanic formation formed from highly differentiated and HFSE-depleted magma, probably in a single volcanic centre of uncertain age. Szentistvánhegy Metavolcanics comprises heterogeneous rocks of a calc-alkaline arc-type suite with wide distribution in a Ladinian chronostratigraphic horizon. Szinva Metabasalt represents within-plate-type alkaline lava flows and adjacent volcaniclastic, mostly peperitic rocks embedded in Carnian platform and basin facies limestone formations. Like the sedimentary formations of the Bükk Mts, rocks of magmatic origin can be correlated with the formations of the South Alpine and Dinaric successions with the significant difference that abundant metavolcanics are not accompanied by intrusive bodies.

Keywords Triassic magmatism · Trace element geochemistry · Stratigraphy · Low grade metamorphism

Introduction

A Middle-Late Triassic Alpine magmatic province was formed during the onset of the Neotethys spreading, with extended and various magmatic formations, e. g. in the Southern Alps, Apennines and Dinarides. Triassic magmatic formations occur also in the Western Carpathians (Hovorka and Spišiak 1988; Harangi et al. 1996), but mostly in the form of redeposited volcaniclastics, dikes, or isolated lava flows only. The Bükk Mts. stands out in this region by a voluminous volcanic complex hosted in sedimentary successions which were correlated to Dinaric analogies (Balogh 1964; Kovács et al. 2000; Less et al. 2005). However, metamorphic overprint and tectonic fragmentation complicate the characterization and distinction of the magmatic formations.

The tectonic fragments were amalgamated during a history involving metamorphism accompanied by ductile

✉ Norbert Németh
foldnn@uni-miskolc.hu

1 Institute of Mineralogy and Geology, University of Miskolc, Miskolc-Egyetemváros, Miskolc H-3515, Hungary

2 Department of Petrology and Geochemistry, Eötvös Loránd University, Budapest, Hungary

3 Institute for Geological and Geochemical Research, Research Centre for Astronomy and Earth Sciences, ELKH, Budaörsi út 45, H-1112 Budapest, Hungary

4 CSFK, MTA Centre of Excellence, Konkoly Thege Miklós út 15-17., H-1121 Budapest, Hungary

5 MTA-ELTE Volcanology Research Group, ELKH, Pázmány Péter sétány 1/C, H-1117 Budapest, Hungary

deformation, other local or regional hydrothermal alterations and large-scale horizontal displacements along fault zones. Because of these processes, rock bodies were dissected and some parts of these extracted from their original environment, while bodies genetically not linked were attached to each other as fault blocks. Syngenetic features often are obscured or obliterated. As bedding contacts also are sheared and often subparallel with major fault zones, stratigraphic continuity remains ambiguous in several cases. The correct interpretation of the genetic relationships is hindered by doubtful stratigraphic and structural positions of the formations.

The Bükk Mts. comprises two major stratigraphic units: Szarvaskő Unit and Paraautochthonous Unit. The Szarvaskő Unit occurs in the western part comprising Triassic and Jurassic oceanic pillow basalt and basic-ultrabasic intrusive bodies. Magmatic interpretation of these rocks is relatively simpler than those of the Paraautochthonous Unit because they retained most of their original textural properties. The white mica K–Ar and zircon fission track cooling ages point also to the Jurassic period (Árkai et al. 1995), with no significant later thermal overprint. These rocks were studied in the past (summarized in Balogh 1964 and Less et al. 2005) and recently (Kiss et al. 2010) from the point of view of magmatic petrography, interpreted as an ophiolitic sequence. Hydrothermal mineral assemblages of these rocks were described by Kiss et al. (2016).

The metavolcanics of the Paraautochthonous Unit are part of carbonate-dominated successions deposited on a continental shelf of the Tethys Ocean, ranging from the Upper Carboniferous to the Middle Jurassic. As the Szarvaskő succession was interpreted to be emplaced as a nappe (Balla 1983; Csontos 1999, although boundaries of this structural unit were never mapped and, therefore, are inferred only), the remaining part is referred to as Paraautochthonous Unit. These metavolcanics have a more diverse mineral and chemical composition than the Szarvaskő ones, but their textures are in several cases strongly overprinted by recrystallization during dynamic deformation processes. White mica K–Ar cooling ages indicate ca. 80 and 120 Ma thermal events with a possible maximal temperature of ~ 350ºC (Árkai et al. 1995). Large variability of the rock types is reflected in the detailed petrographic studies of Szentpétery (1923, 1929a, b, 1931, 1932, 1934a, b, 1935, 1936, 1937, 1950a, b) and the mapping of Pantó (1951). It was also noticed that bulk rock composition was changed, and major element geochemistry does not show the original magmatic composition (Mezősi 1950; Balogh 1964; Harangi et al. 1996). This situation was interpreted as low-grade, pumpellyite–prehnite or pumpellyite–actinolite facies regional metamorphism of a calc-alkaline stratovolcanic suite and alkaline within-plate basalts (Árkai 1973, 1983; Dobosi 1986; Szoldán 1990; Harangi et al. 1996). Modern studies, however, were restricted to few localities not representing the multitude of rock varieties. Explorations (including drilling) related to the mapping project of the Hungarian Geological Institute were done in the 1990s (Velledits 1999; Pelikán 1999; Less et al. 2005). A shear zone in metavolcanics at Lillafüred was studied in detail by Koroknai et al. (2008). Local hydrothermal mineralizations were also studied at some special occurrences (Balogh 1964; Kubovics et al. 1989; Szakáll and Földvári 1995; Szakáll et al. 2012; Szabó and Vincze 2013; Zajzon et al. 2014; Ozdín and Szakáll 2014; Fehér 2015; Németh et al. 2015, 2016; Gál et al. 2022).

In this paper we present the results of geochemical-mineralogical testing of the metavolcanics bodies of the Paraautochthonous Unit. The study covers several occurrences which were not sampled and tested before, and several metamorphic or altered rock types of assumed magmatic origin. Considering all properties, relict minerals and trace elements not mobilized by post-magmatic processes can be used as indicators of synmagmatic relationships of the lithological units. Mineral assemblage alone is not enough to discriminate the rock types of the formations. Instead, trace element composition was found appropriate to discriminate the formations and, corresponding to this, petrographic characteristics of these formations were observed. We provide a basis for determination of stratigraphic units of magmatic origin within the Paraautochthonous successions of the Bükk Mts.

Applied methods

The study of the metavolcanics bodies was based on reambulation, and in most cases mapping of the outcrops. Rock samples were collected mostly from the surface, with exceptions of 5 drillcore and 1 trench samples of a previous exploration (Szabó and Vincze 2013) from the store of the Mecsekérc Co. In the sampling strategy we concentrated on covering as many of the available metavolcanics bodies and supposed types as we could afford, involving the outcrops of those rock bodies which lacked previous data, with ca. 150 new samples in general. Samples for detailed measurements were chosen to be representative for these bodies; small bodies are represented by one or two samples only. Metavolcanics are mingled with sediments in several cases, so some samples of probable mixed or redeposited origin were also included. Phyllosilicate-dominated rock varieties of the formations are probably underrepresented in our samples because these rocks are less resistant to the weathering and yield mostly small-grained debris at the outcrops only. Sampling was supported by radiometric mapping of potassium, thorium, and uranium concentrations (Németh et al. 2015, 2016).

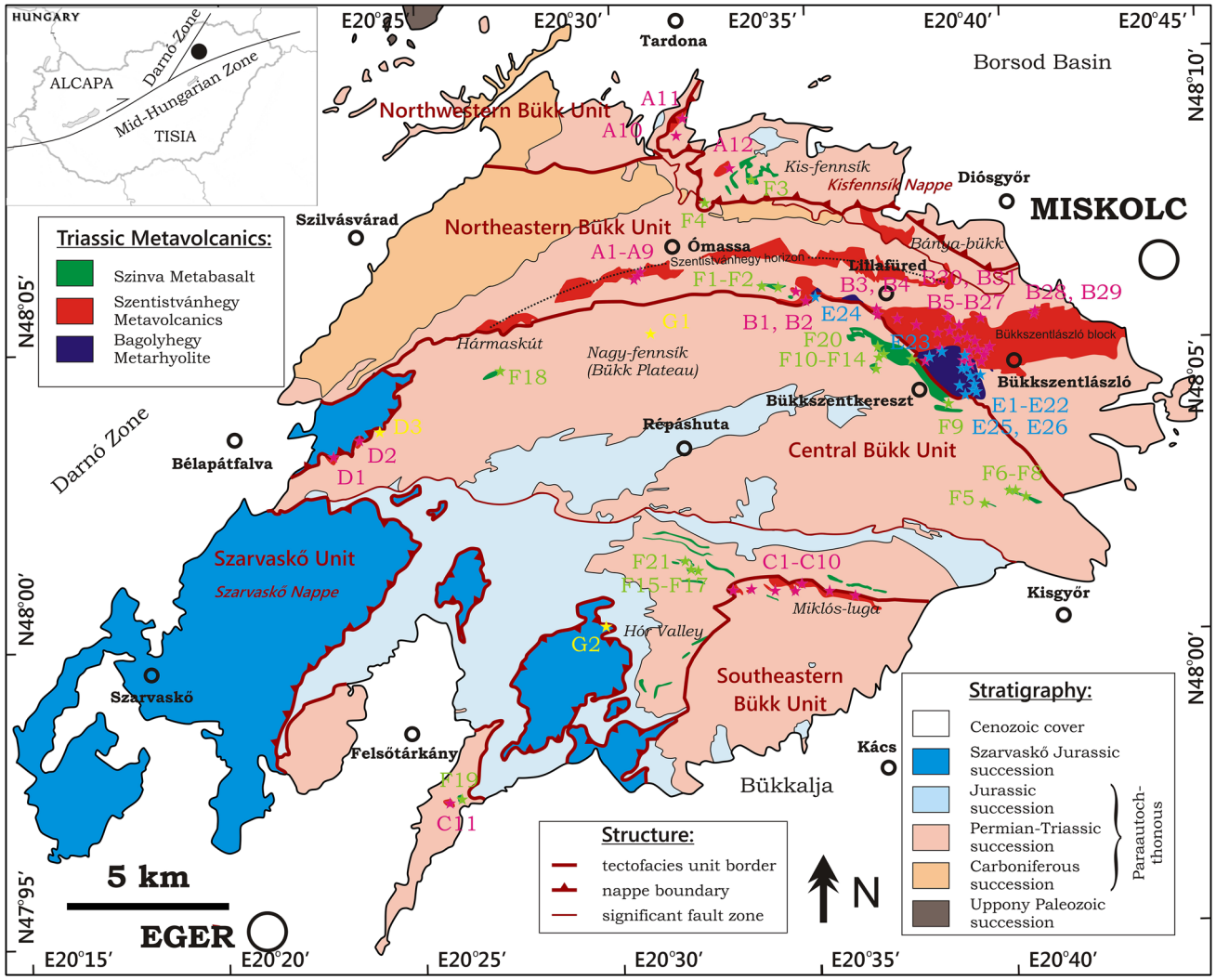

Fig. 1 Geological outlines of the Bükk Mts. with the outcrops of metavolcanics in the Paraautochthonous successions. Contours constructed using maps of Balogh (1964) and Less et al. (2005), modified by own mapping results. Sampling sites are marked with stars: olive – Szinva Metabasalt, magenta – Szentistvánhegy Metavolcanics, cyan – Bagolyhegy Metarhyolite, yellow – other samples. Overlapping symbols were omitted

The laboratory measurements of geochemical composition used in this study were made on 100 samples altogether, 97 samples from metavolcanic formations of the Bükk Paraautochthonous successions and 3 further samples which were also supposed to possibly belong here but proved to be of other origin (see Appendix A). Sampling sites are shown in Fig. 1, and coordinates (EOV, Hungarian National Projection System) are given in Table 1. Geochemical composition of pulverized and homogenized samples was assayed using an Elan DRC II. Perkin Elmer ICP-MS and an Ultima-2C Jobin Yvon ICP-OES devices after Li-borate digestion, followed by acidic dissolution in the laboratory of the Geological and Geophysical Institute of Hungary (MFGI) in the CriticEl project made by the University of Miskolc, and by standard lithogeochemical ICP-AES major element and ICP-MS trace element analysis in later assays by accredited laboratories (ALS and Bureau Veritas). Additional elements in samples lacking some data because of incomplete assays were analysed by wavelength dispersive X-ray fluorescence using a Rigaku Supermini 200 WDXRF machine (Pd-tube of 200 W power, 50 kV, 4 mA, 4 g pressed pellet, ZSX software) in the University of Miskolc, Institute of Mineralogy and Geology. Zr and TiO_2 concentration analyses playing key role in the interpretation were made on 20 samples both by ICP and WDXRF, and the calculated linear correlation coefficient of these datasets is 0.99 (Zr) and 0.90 (TiO_2). Assay results are summarized in Table 1. Volatiles were not assayed; presence of these

Table 1 Chemical composition of the assayed samples

sample id	Y	X	SiO_2	Al_2O_3	TiO_2	Fe_2O_3	MnO	MgO	CaO	Na_2O	K_2O	P_2O_5	BaO	SrO	Cr_2O_3	Total ox.	LOI
	EOV (Hungarian National Projection)		wt%	wt%	wt%	wt%	wt%	wt%	wt%	wt%	wt%	wt%	wt%	wt%	wt%	wt%	wt%
Detection limit			0,10	0,1	0,02	0,03	0,003	0,15	0,03	0,03	0,2	0,15	0,005	0,0002			
Detection limit			0,01	0,01	0,01	0,01	0,010	0,01	0,01	0,01	0,01	0,01	0,010	0,010	0,002		0,01
Detection limit			0,01	0,01	0,01	0,04	0,010	0,01	0,01	0,01	0,01	0,01			0,002		-5,10
Detection limit			0,10	0,1	0,01	0,01	0,005	0,01	0,01	0,01	0,01	0,005					
Szentistvánhegy Metavolcanics																	
A1	759070	307490	64,90	14,80	0,48	3,38	0,070	1,24	4,57	3,66	1,91	0,11		b.d.l.	0,002	95,12	5,02
A2	759080	307540	65,00	17,00	0,96	5,04	0,070	1,07	1,25	2,80	3,10	0,19		b.d.l.	0,014	96,49	3,18
A3	759105	307570	63,70	17,20	0,92	5,06	0,090	1,27	2,49	3,19	3,03	0,17		b.d.l.	0,013	97,13	3,90
A4	759110	307600	65,30	16,90	0,95	5,41	0,090	1,42	0,75	3,71	2,44	0,19		b.d.l.	0,013	97,17	2,99
A5	759120	307640	70,90	14,55	0,80	3,80	0,060	1,20	0,60	3,01	1,97	0,14		b.d.l.	0,011	97,04	2,85
A6	759160	307690	57,10	17,55	1,04	6,16	0,080	2,59	3,90	2,89	1,95	0,18		0,010	0,042	93,49	6,02
A7	759225	307710	61,00	16,75	1,03	6,48	0,090	2,60	2,77	3,29	1,79	0,18		b.d.l.	0,039	96,02	5,21
A8	759270	307730	56,50	17,75	0,94	4,73	0,070	1,71	5,58	3,68	1,79	0,16		b.d.l.	0,019	92,93	6,81
A9	759280	307750	57,30	17,90	0,86	5,73	0,550	2,71	4,63	2,63	1,86	0,14		0,010	0,014	94,33	6,54
A10	760390	311980	65,85	16,47	1,25	3,84	0,040	0,40	3,01	4,12	3,13	0,24			0,005	98,36	1,50
A11	760697	312369	67,10	13,30	0,70	7,59	0,113	0,80	0,93	4,16	2,01	0,20	0,029	0,014		96,95	
A12	762047	310969	70,20	13,40	0,56	4,38	0,056	1,13	0,57	2,91	4,08	b.d.l.	0,061	0,010		97,35	
B1	764406	306839	64,40	17,60	0,69	3,83	0,118	0,80	1,95	6,85	0,31	0,23	0,012	0,030		96,83	
B2	764107	307141	56,90	18,50	0,57	5,86	0,270	3,36	2,48	1,29	9,84	0,14		0,020	0,009	99,24	2,54
B3	766650	306410	72,67	15,07	0,25	1,53	0,020	0,58	0,06	1,83	6,02	0,03			b.d.l.	98,06	1,80
B4	766626	306559	55,60	18,10	1,28	8,15	0,113	3,03	6,02	1,16	2,19	0,15	0,042	0,056		95,89	
B5	769915	305125	74,10	12,60	0,37	2,22	0,020	b.d.l.	0,04	4,78	4,52	b.d.l.	0,064	0,013		98,72	
B6	769760	305320	62,00	16,60	0,38	4,09	0,062	0,56	0,28	3,23	4,77	0,10	0,077	0,015		92,16	
B7	769420	305700	72,10	14,60	0,27	1,13	0,014	0,19	0,07	3,23	6,23	0,04	0,104	0,014		97,99	
B8	769460	305700	56,80	14,20	1,71	8,47	0,150	3,70	1,88	4,09	1,86	0,19	0,030	0,020		93,10	
B9	769660	305540	65,40	11,90	0,73	9,35	0,120	2,75	2,14	1,41	0,81	0,28	0,020	0,020	0,020	94,95	3,56
B10	769660	305600	61,60	15,10	0,53	3,68	0,067	1,94	2,20	1,82	5,55	0,08	0,086	0,030		92,68	
B11	769850	304970	69,00	16,10	0,46	2,39	0,024	0,29	0,30	3,57	6,53	b.d.l.	0,081	0,010		98,76	
B12	769860	306298	70,80	15,60	0,54	1,81	0,004	b.d.l.	0,10	9,22	0,58	0,05	0,011	0,010		98,72	
B13	768830	306330	73,00	13,70	0,44	1,72	0,023	0,20	0,48	2,78	5,92	0,14	0,117	0,015		98,53	
B14	768495	305897	77,20	11,80	0,36	1,41	0,013	0,23	0,09	3,97	3,91	b.d.l.	0,094	0,009		99,09	
B15	769530	304845	73,80	11,90	0,42	3,77	0,090	0,96	0,67	4,20	1,81	0,22	0,078	0,010		97,92	
B16	769435	305040	72,70	14,00	0,35	2,60	0,041	0,55	0,98	5,52	1,38	b.d.l.	0,046	0,013		98,17	
B17	769475	305280	69,90	15,70	0,37	2,59	0,030	0,69	0,61	4,58	3,06	b.d.l.	0,087	0,013		97,63	
B18	769980	305248	58,40	17,00	1,12	7,12	0,100	3,13	4,26	1,17	1,55	b.d.l.	0,747	0,036		94,63	
B19	769133	305655	61,50	20,87	0,58	2,00	0,020	0,45	0,05	4,13	8,38	0,04			b.d.l.	98,02	1,70
B20	767850	306080	58,95	17,53	1,47	6,91	0,070	1,56	4,08	6,26	0,11	0,27			0,006	97,22	2,60
B21	768589	305345	47,50	24,81	1,44	8,12	0,030	2,42	1,47	0,54	7,36	0,07			0,024	93,78	6,10
B22	769366	304935	55,12	20,47	0,89	7,12	0,110	2,60	3,94	3,02	3,03	0,19			0,014	96,50	3,30
B23	769760	305320	57,91	20,69	0,62	5,58	0,040	2,62	1,17	1,25	5,95	0,09			b.d.l.	95,92	3,90
B24[c]	768150	304974	59,08	16,59	1,01	7,90	0,070	4,57	0,96	3,41	2,18	0,20			0,036	96,01	3,80
B25	770060	305175	71,02	15,53	0,34	1,13	b.d.l.	0,09	0,22	4,38	6,19	0,09			b.d.l.	98,99	0,80
B26	768886	305835	57,29	17,16	1,50	7,99	0,070	4,35	2,00	5,21	0,91	0,20			0,006	96,69	3,10
B27	769185	306025	55,63	18,34	0,82	3,91	0,060	2,38	5,70	1,62	4,88	0,29			0,011	93,64	6,10
B28	771590	306560	64,12	16,14	0,80	5,27	0,050	2,07	1,39	3,79	2,63	0,17			0,008	96,44	3,30
B29	771510	306460	56,90	23,80	1,14	2,07	0,200	1,02	b.d.l.	1,53	6,87	0,02	0,117	0,004		93,67	
C1	765965	297679	51,60	14,90	1,02	5,84	0,054	2,85	5,78	1,15	6,79	0,16	0,026	0,006		90,17	
C2	765145	297819	56,40	17,50	0,88	6,20	0,037	3,93	0,25	0,86	8,65	b.d.l.	0,017	0,002		94,73	
C3	764890	297870	52,80	14,50	0,95	7,05	0,040	2,73	0,32	0,20	9,03	0,14				87,76	
C4	764290	298040	53,30	17,80	1,35	5,67	0,030	3,27	0,48	3,50	2,28	0,21	0,029	0,011		87,93	
C5	764120	297830	60,50	14,80	0,60	4,63	0,050	2,51	0,38	0,49	6,55	0,13	0,037	0,006		90,68	
C6	764080	297840	56,10	16,70	0,77	3,28	0,030	2,18	1,20	2,23	3,62	0,10	0,038	0,015		86,26	
C7	763460	297830	59,30	15,10	1,16	5,52	0,020	3,55	0,65	0,51	4,55	0,22	0,022	0,003		90,61	
C8	762730	297875	55,00	17,50	1,04	5,36	0,010	2,92	0,13	0,17	8,50	0,05	0,020	0,003		90,70	
C9	762730	297875	58,07	18,35	0,96	4,89	0,020	2,57	0,25	0,33	10,03	0,08			0,009	95,56	4,30
C10	762160	297840	64,10	16,80	0,29	2,94	0,010	2,57	0,17	0,04	5,14	0,07	0,050	0,001		92,18	
C11	753362	291228	65,29	14,46	0,76	5,89	0,040	3,18	0,31	3,63	0,45	0,05			0,013	94,07	5,70
D1	749746	301968	55,67	17,38	1,90	9,75	0,040	4,82	0,36	1,50	2,75	b.d.l.			0,008	94,18	5,70
D2	750545	302487	66,67	11,67	1,22	8,47	0,050	3,88	1,44	0,27	1,26	0,06			0,006	95,00	4,90

sample id	Be	Sc	V	Cr	Co	Ni	Cu	Zn	Ga	Ge	As	Se
	ppm	ppm	ppm	ppm	ppm	ppm	ppm	ppm	ppm	ppm	ppm	ppm
Detection limit	0,50	0,50	2,50		0,50	1,00		0,25		0,25	1,50	1,00
Detection limit			5,00	10,00					0,10			
Detection limit	1,00	1,00	8,00		0,20	20,00			0,50			
Detection limit												
Szentistvánhegy Metavolcanics												
A1			31,00	20,00					21,90			
A2			102,00	120,00					21,70			
A3			101,00	110,00					21,80			
A4			97,00	120,00					21,60			
A5			83,00	100,00					17,60			
A6			132,00	360,00					19,70			
A7			113,00	340,00					21,00			
A8			106,00	160,00					19,70			
A9			106,00	120,00					20,00			
A10	2,00	13,00	60,00		4,50	b.d.l.			18,50			
A11	3,64	16,10			7,49				15,40	0,98	11,00	
A12	2,56	13,20			9,26				15,50	0,87	8,20	
B1	2,40	11,50			7,47				13,70	1,29	4,89	
B2			110,00	80,00					20,80			
B3	4,00	16,00	12,00		1,70	b.d.l.			21,40			
B4	3,16	17,00			16,70				20,70	1,14	13,20	
B5	1,76	8,80			2,11				11,30	0,97	11,00	
B6	4,55	23,80			8,32	16,10	20,10	36,20	21,70	0,73	38,10	
B7	0,79	8,50			1,17				14,20	0,49	10,70	
B8	2,07	20,90			12,90				14,50	0,43	9,28	
B9	2,66	12,40	74,00	150,00	17,40				22,10	0,75	10,50	
B10	1,98	14,30			10,90				16,00	0,34	7,82	
B11	2,10	8,33			4,00				9,65	0,93	11,10	
B12	1,60	7,39			4,73				9,84	0,59	21,20	
B13	1,44	9,12			4,35				14,50	0,57	11,20	
B14	0,98	7,11			2,88				14,50	0,47	9,34	
B15	2,39	10,60			6,06				14,90	0,84	18,60	
B16	2,59	6,68			3,28				13,60	0,78	12,20	
B17	3,54	9,02			4,66				20,30	0,77	16,10	
B18	1,73	15,90			13,10				22,40	1,02	6,34	
B19	b.d.l.	28,00	53,00		0,30	b.d.l.			37,30			
B20	b.d.l.	26,00	105,00		8,00	b.d.l.			19,30			
B21	8,00	32,00	85,00		16,60	51,00			24,80			
B22	4,00	19,00	105,00		14,90	35,00			25,00			
B23	2,00	19,00	20,00		2,60	b.d.l.			29,70			
B24[c]	3,00	21,00	139,00		20,30	38,00			18,80			
B25	1,00	11,00	9,00		0,60	b.d.l.			10,80			
B26	2,00	26,00	133,00		15,40	b.d.l.			17,70			
B27	2,00	19,00	72,00		7,70	b.d.l.			22,20			
B28	2,00	16,00	118,00		1,00	b.d.l.			19,20			
B29	4,36	22,00			9,07				28,20	0,59	36,10	
C1	1,65	17,70			15,60				15,20	0,64	7,79	
C2	1,61	13,00			15,60				15,90	0,70	4,69	
C3	1,42	17,00	135,00		24,80		18,00				2,41	
C4	3,25	22,90	111,00		12,90	28,40	13,60				3,00	
C5	1,01	7,79	64,50		12,20		12,10				2,22	
C6	1,13	10,80	110,00		11,00		11,10				2,02	
C7	2,90	17,80	112,00		21,20		27,40				b.d.l.	
C8	1,37	17,00	105,00		15,60	54,90	6,20				1,95	
C9	3,00	18,00	84,00		8,70	b.d.l.			19,40			
C10	3,11	8,60	46,40		b.d.l.	b.d.l.	5,92				2,67	
C11	b.d.l.	12,00	41,00		11,60	32,00			16,40			
D1	2,00	28,00	59,00		16,00	b.d.l.			20,90			
D2	3,00	18,00	23,00		12,10	b.d.l.			13,20			

sample id	Rb	Sr	Y	Zr	Nb	Sn	Sb	Cs	Ba	La	Ce	Pr	Nd	Sm	Eu
	ppm	ppm	ppm	ppm	ppm	ppm	ppm	ppm	ppm	ppm	ppm	ppm	ppm	ppm	ppm
Detection	0,25		0,25	0,25	0,25	0,50	0,10	0,25		0,25	0,25	0,10	0,10	0,10	0,05
Detection	0,20	0,10	0,10	2,00	0,20	1,00		0,01	0,50	0,10	0,10	0,03	0,10	0,03	0,03
Detection	0,10	0,50	0,10	0,10	0,10	1,00		0,10	1,00	0,10	0,10	0,02	0,30	0,05	0,02
Detection	10,00			10,00					10,00						
Szentistvánhegy Metavolcanics															
A1	79,00	150,00	43,50	311,00	9,80	7,00		2,42	342,00	35,20	74,90	9,10	36,90	7,65	1,01
A2	133,50	130,00	37,80	239,00	10,50	5,00		7,32	377,00	30,50	61,90	8,39	34,30	7,63	1,19
A3	139,50	156,50	39,40	256,00	10,40	4,00		7,47	356,00	31,30	64,40	8,12	33,50	7,10	1,20
A4	111,00	119,00	35,50	261,00	11,60	5,00		5,90	324,00	25,70	57,50	6,89	28,20	6,36	1,02
A5	79,40	150,00	31,40	222,00	9,40	6,00		3,61	289,00	22,90	50,30	6,00	25,20	5,80	1,04
A6	72,70	173,00	29,30	192,00	7,20	4,00		2,87	250,00	20,50	42,60	5,71	24,00	5,46	1,16
A7	55,50	135,50	31,50	207,00	7,60	3,00		2,31	277,00	17,70	39,40	5,18	22,60	5,20	1,19
A8	62,20	164,50	26,30	170,00	6,80	4,00		6,73	184,50	16,80	37,70	4,85	20,60	4,71	1,04
A9	68,90	200,00	25,80	154,00	7,00	4,00		6,57	203,00	16,00	35,40	4,54	18,60	4,39	1,10
A10	118,50	200,80	31,20	272,20	11,00	2,00		4,70	414,00	29,50	60,00	7,51	30,10	6,25	1,11
A11	64,40		39,50	322,00	13,10	10,60		2,17		41,30	83,10	10,10	37,20	7,64	1,01
A12	85,80		36,70	340,00	14,40	9,52		2,06		41,10	59,40	9,42	34,00	6,91	1,12
B1	13,60		42,60	415,00	15,30	6,41		1,08		51,20	101,00	17,60	53,20	10,20	1,07
B2	248,00		32,70	151,00	10,90	8,00		3,49	675,00	22,00	48,00	5,64	23,60	5,60	1,48
B3	206,80	90,90	45,90	294,80	12,80	9,00		8,20	590,00	34,90	60,50	8,60	31,10	6,41	0,32
B4	83,20		30,90	209,00	15,20	5,04		4,88		44,00	82,00	10,10	37,40	7,64	1,76
B5	100,00		17,50	421,00	10,20	1,01		4,73		16,70	24,30	2,37	6,49	1,11	0,36
B6	167,00		53,10	495,00	14,50	10,00		12,10	757,00	47,60	97,50	12,20	46,50	10,20	0,95
B7	160,00		25,10	362,00	10,40	4,62		6,60	868,00	30,40	56,20	6,65	22,90	4,42	0,58
B8	81,00		30,10	182,00	9,13	2,77		8,81	357,00	22,80	41,20	6,03	24,90	5,96	1,22
B9	53,70	188,50	42,70	235,00	13,60	12,00		4,17	160,00	39,80	76,00	9,88	39,10	7,30	1,21
B10	159,00		21,80	232,00	10,00	8,19		9,17		24,20	33,50	4,00	15,30	3,41	0,90
B11	172,00		28,60	359,00	11,20	6,10		8,31	553,00	28,50	55,50	6,74	25,90	5,78	0,78
B12	12,60		21,60	322,00	11,00	4,60		0,72		22,40	43,30	5,03	18,30	3,67	0,45
B13	134,00		23,40	295,00	11,80	10,00		6,69		37,30	71,50	8,50	30,80	6,08	0,96
B14	86,20		25,70	425,00	12,60	11,20		3,89	482,00	17,40	28,00	3,43	12,10	2,67	0,53
B15	83,80		43,70	326,00	11,50	4,21		8,49		43,90	77,40	10,90	42,30	9,74	1,20
B16	51,00		41,70	434,00	11,40	5,06		5,50		40,30	73,20	9,68	37,40	8,27	0,84
B17	101,00		38,90	553,00	14,40	6,40		13,40		31,30	53,90	7,78	27,70	6,14	0,84
B18	119,00		18,70	201,00	13,30	2,90		9,09		30,30	58,90	6,97	25,50	5,38	3,41
B19	294,30	114,10	28,60	804,20	22,20	14,00		16,40	859,00	18,90	36,50	4,07	13,70	2,58	0,21
B20	3,60	206,00	46,80	296,50	14,40	4,00		0,70	23,00	41,70	77,30	10,18	39,90	8,45	1,48
B21	416,80	71,40	29,50	219,10	13,60	4,00		46,90	227,00	46,50	94,20	10,62	39,90	7,45	1,64
B22	175,30	391,80	51,60	307,00	14,10	5,00		14,10	336,00	47,40	89,20	10,59	40,20	8,52	1,42
B23	362,10	170,20	60,70	660,00	17,70	8,00		33,20	327,00	48,80	101,00	12,44	48,00	10,93	1,19
B24[c]	124,40	57,70	26,90	187,80	11,60	2,00		11,20	269,00	29,20	55,50	6,43	24,60	5,01	1,10
B25	134,30	113,30	37,60	477,50	12,60	5,00		6,50	1106,00	30,80	56,80	7,52	28,20	6,30	0,41
B26	70,80	156,70	30,20	233,10	11,00	3,00		7,00	300,00	25,40	56,40	6,81	28,00	6,13	1,28
B27	144,60	120,20	70,80	387,80	16,20	7,00		17,40	269,00	54,70	101,20	13,09	53,30	13,27	1,12
B28	165,00	128,40	35,70	363,10	13,60	7,00		12,40	448,00	23,50	47,70	6,16	24,50	6,15	0,67
B29	138,00		12,30	289,00	14,00	4,61		6,51	1019,00	3,05	4,04	0,46	1,80	0,53	0,56
C1	113,00		15,70	126,00	8,56	2,50		4,25		15,10	30,00	3,87	15,20	3,34	0,90
C2	140,00		14,60	138,00	6,95	2,20		6,56		11,50	27,80	2,58	9,92	2,11	0,59
C3	134,00		14,90	123,00	6,53	b.d.l.	0,35	5,49	263,00	12,30	34,30	3,55	13,90	3,01	0,69
C4	40,40		57,40	465,00	20,00	7,44	0,38	3,39	68,00	47,20	95,80	12,30	48,00	10,30	1,18
C5	80,00		13,40	104,00	4,59	b.d.l.	0,32	3,67	220,00	17,10	36,00	4,38	17,00	3,36	0,94
C6	58,80		17,10	162,00	6,50	b.d.l.	0,35	2,65	228,00	16,20	35,30	4,53	17,70	4,07	0,83
C7	96,20		30,80	251,00	12,90	3,27	0,37	12,80	b.d.l.	32,00	65,20	8,35	32,80	6,96	0,96
C8	121,00		12,90	162,00	7,25	b.d.l.	0,34	4,98	b.d.l.	15,00	25,40	3,36	12,60	2,29	0,50
C9	120,00	63,50	14,00	165,00	6,90	2,00		5,30	298,00	18,40	32,60	3,91	14,10	2,65	0,73
C10	80,70		28,80	265,00	12,60	5,88	0,28	5,05		28,50	79,70	6,56	23,60	4,66	0,66
C11	8,80	118,70	15,00	269,40	9,70	2,00		1,40	1355,00	21,50	39,60	5,33	19,40	3,85	0,66
D1	87,60	34,50	28,30	248,00	10,80	3,00		3,30	217,00	25,20	53,20	6,75	26,70	5,70	1,20
D2	46,20	37,50	21,20	166,80	7,70	2,00		2,50	154,00	15,40	31,80	4,07	16,40	4,12	0,99

sample id	Gd	Tb	Dy	Ho	Er	Tm	Yb	Lu	Hf	Ta	W	Tl	Th	U
	ppm	ppm	ppm	ppm	ppm	ppm	ppm	ppm	ppm	ppm	ppm	ppm	ppm	ppm
Detection	0,10	0,10	0,10	0,10	0,10	0,10	0,10	0,10		0,25	0,25	0,10	0,25	0,25
Detection	0,05	0,01	0,05	0,01	0,03	0,01	0,03	0,01	0,20	0,10	1,00		0,05	0,05
Detection	0,05	0,01	0,05	0,02	0,03	0,01	0,05	0,01	0,10	0,10	0,50		0,20	0,10
Detection														
Szentistvánhegy Metavolcanics														
A1	7,96	1,21	7,28	1,48	4,79	0,69	4,50	0,65	8,20	0,70	9,00		13,60	3,58
A2	7,49	1,14	6,80	1,31	3,97	0,54	3,74	0,54	7,10	0,70	12,00		10,30	2,41
A3	6,97	1,09	6,79	1,31	3,82	0,57	3,64	0,51	6,80	0,80	22,00		10,20	2,36
A4	6,27	0,99	6,14	1,19	3,84	0,57	3,91	0,50	7,20	0,80	17,00		10,15	2,32
A5	5,55	0,89	5,66	1,09	3,28	0,47	3,19	0,52	6,20	0,60	9,00		8,96	2,31
A6	5,72	0,81	5,37	1,04	2,92	0,46	2,85	0,43	5,30	0,50	18,00		6,30	1,71
A7	5,44	0,90	5,69	1,10	3,55	0,51	3,17	0,49	5,20	0,50	7,00		6,64	2,19
A8	4,90	0,75	4,94	0,93	2,79	0,41	2,73	0,41	4,50	0,40	14,00		5,69	1,43
A9	4,54	0,74	4,32	0,82	2,68	0,39	2,40	0,39	4,10	0,40	14,00		5,51	1,31
A10	6,24	0,96	5,34	1,07	2,92	0,40	2,45	0,37	6,70	0,80	1,70		10,30	1,10
A11	6,71	1,26	7,31	1,61	4,70	0,73	4,68	0,75		1,22	2,58	0,29	14,90	2,96
A12	5,93	1,10	6,33	1,34	4,05	0,62	4,05	0,64		1,17	2,18	0,32	11,70	3,03
B1	9,25	1,52	8,47	1,73	4,53	0,66	4,14	0,65		1,30	2,35	0,15	18,50	3,50
B2	6,12	0,93	5,98	1,10	3,53	0,44	3,27	0,47	4,60	0,70	26,00		13,35	2,46
B3	6,06	1,05	6,61	1,49	5,03	0,75	4,92	0,79	8,30	1,00	2,80		22,80	6,20
B4	6,74	1,19	6,66	1,32	3,64	0,55	3,26	0,49		1,21	1,38	0,63	11,60	2,44
B5	1,29	0,24	2,03	0,63	2,38	0,43	2,94	0,46		0,83	2,19	0,85	11,70	3,31
B6	9,05	1,63	9,68	2,08	5,91	0,99	6,15	0,97		1,26	3,41	0,91		5,80
B7	3,51	0,65	4,18	1,02	3,10	0,53	3,50	0,57		1,39	2,55	1,24		3,56
B8	5,38	0,97	5,74	1,20	3,19	0,47	2,91	0,43		0,82	1,23	0,48		1,58
B9	7,18	1,11	6,96	1,27	3,64	0,57	3,35	0,59	5,60	1,30	6,00	0,34	11,85	6,43
B10	3,16	0,60	3,61	0,86	2,62	0,42	2,83	0,48		0,93	2,41	1,27		2,79
B11	4,78	0,93	5,37	1,19	3,55	0,55	3,62	0,53		0,99	2,26	0,87	15,10	2,88
B12	3,11	0,59	3,88	0,91	2,66	0,42	2,73	0,41		0,93	2,36	0,40	12,90	3,76
B13	4,67	0,84	4,67	0,98	2,88	0,46	3,13	0,51		1,00	1,61	1,05	15,70	4,16
B14	2,80	0,63	4,40	1,03	3,26	0,54	3,59	0,56		1,07	4,98	0,54	13,30	3,49
B15	8,12	1,48	8,35	1,75	4,78	0,70	4,43	0,68		0,90	1,90	0,41	14,20	3,27
B16	6,77	1,32	7,63	1,58	4,51	0,69	4,18	0,64		1,07	4,94	0,31	15,20	3,77
B17	5,15	1,08	7,12	1,54	4,78	0,74	5,10	0,80		1,23	2,16	0,74	18,80	4,65
B18	4,20	0,74	4,18	0,84	2,34	0,35	2,18	0,34		1,11	1,03	0,52	10,90	1,85
B19	2,42	0,46	3,40	0,97	3,84	0,68	5,10	0,95	19,70	1,70	5,70		22,50	7,90
B20	8,54	1,37	8,42	1,67	4,86	0,69	4,41	0,69	7,30	1,10	2,40		14,80	4,00
B21	6,67	1,04	5,72	1,05	2,74	0,40	2,45	0,37	5,40	1,00	1,10		11,90	3,00
B22	8,61	1,39	8,27	1,78	4,94	0,71	4,38	0,70	7,90	1,10	2,10		16,00	3,60
B23	11,24	1,83	10,95	2,23	6,56	0,84	5,20	0,74	16,10	1,40	2,70		24,40	6,00
B24[c]	4,90	0,82	4,82	1,02	2,90	0,40	2,64	0,42	4,60	0,80	1,20		9,90	6,10
B25	6,23	1,11	7,05	1,45	4,63	0,69	4,49	0,67	11,80	1,00			18,70	6,70
B26	6,34	1,00	5,78	1,22	3,44	0,50	3,15	0,49	5,80	1,00			8,10	2,00
B27	14,44	2,48	15,57	3,09	8,97	1,24	8,13	1,22	9,50	1,10			17,90	7,80
B28	6,03	1,02	6,37	1,34	4,31	0,58	4,04	0,64	8,80	1,10			16,30	6,20
B29	0,65	0,19	1,66	0,48	1,72	0,32	2,22	0,36		1,13	7,29	3,12	10,50	2,88
C1	2,90	0,52	2,96	0,63	1,85	0,29	1,84	0,29		0,81	1,01	0,91	5,31	0,24
C2	1,89	0,38	2,63	0,63	1,96	0,33	2,19	0,36		0,65	0,70	0,86	5,82	0,26
C3	2,83	0,50	3,13	0,67	2,00	0,30	1,89	0,28		0,62	2,12		5,62	b.d.l.
C4	9,00	1,65	10,60	2,30	6,77	1,04	6,83	1,08		1,62	2,40		20,80	4,84
C5	2,91	0,48	2,79	0,58	1,69	0,26	1,66	0,26		0,56	13,80		4,70	b.d.l.
C6	3,65	0,64	3,61	0,75	2,11	0,31	1,91	0,28		0,64	2,95		5,06	1,73
C7	5,91	1,02	6,01	1,21	3,39	0,49	3,13	0,48		0,99	1,79		11,30	2,30
C8	1,88	0,34	2,27	0,52	1,67	0,28	1,94	0,32		0,71	3,09		6,32	b.d.l.
C9	2,35	0,37	2,51	0,50	1,49	0,22	1,26	0,20	4,00	0,40	1,00		6,10	1,30
C10	4,18	0,77	5,00	1,11	3,35	0,51	3,38	0,53		1,30	2,21		30,30	8,08
C11	3,51	0,55	3,20	0,56	1,49	0,19	1,18	0,17	5,80	0,70	3,10		6,90	2,50
D1	5,67	0,89	5,44	1,07	3,15	0,43	2,96	0,43	6,10	0,80	0,60		9,80	0,60
D2	4,57	0,75	4,38	0,85	2,26	0,31	2,09	0,30	4,10	0,50	1,30		6,30	0,40

Table 1 (continued)

sample id	Y	X	SiO_2	Al_2O_3	TiO_2	Fe_2O_3	MnO	MgO	CaO	Na_2O	K_2O	P_2O_5	BaO	SrO	Cr_2O_3	Total ox.	LOI	Be	Sc	V	Cr	Co	Ni	Cu	Zn	Ga	Ge	As	Se
	EOV (Hungarian National Projection)		wt%	wt%	wt%	wt%	wt%	wt%	wt%	wt%	wt%	wt%	wt%	wt%	wt%	wt%	wt%	ppm	ppm	ppm	ppm	ppm	ppm	ppm	ppm	ppm	ppm	ppm	ppm
Detection limit			0,10	0,1	0,02	0,03	0,003	0,15	0,03	0,03	0,2	0,15	0,005	0,0002				0,50	0,50	2,50		0,50	1,00		0,25		0,25	1,50	1,00
Detection limit			0,01	0,01	0,01	0,01	0,010	0,01	0,01	0,01	0,01	0,01	0,010	0,010	0,002		0,01			5,00	10,00					0,10			
Detection limit			0,01	0,01	0,01	0,04	0,010	0,01	0,01	0,01	0,01	0,01			0,002		-5,10	1,00	1,00	8,00		0,20	20,00			0,50			
Detection limit			0,10	0,1	0,01	0,01	0,005	0,01	0,01	0,01	0,01	0,005																	
Bagolyhegy Metarhyolite																													
E1	769530	304480	72,80	14,30	0,06	1,75	0,085	0,69	0,56	2,86	3,97	0,34	b.d.l.	0,002		97,42		9,92	3,00	5,17		0,68	1,93	20,80	45,00	18,40	0,31	16,00	50,20
E2	769530	304470	73,70	13,89	0,04	1,47	0,030	0,50	0,52	2,00	5,99	0,35			b.d.l.	98,49	1,40	2,00	3,00	b.d.l.		0,40	b.d.l.			20,30			
E3	769540	304530	77,30	12,30	0,04	1,40	0,121	0,43	0,22	2,44	3,87	b.d.l.	0,005	0,004		98,14		5,92	2,17	b.d.l.		9,66	b.d.l.	15,10	54,60	13,50	b.d.l.	15,40	55,00
E4	769620	304070	79,10	11,40	0,04	1,60	0,029	0,24	0,22	2,59	3,84	0,17	0,006	0,007		99,24		3,52	2,62			b.d.l.				8,81	b.d.l.	47,40	
E5	769310	304100	78,40	11,30	0,06	1,08	0,012	b.d.l.	0,34	4,60	3,75	0,15	0,007	0,012		99,71		1,90	1,38			b.d.l.				15,40	0,55	25,80	
E6	769360	305180	74,40	11,70	0,06	1,04	0,040	0,08	0,16	1,08	8,64	0,08	b.d.l.	b.d.l.	0,020	97,30	0,57	2,49	3,08	8,00	210,00	b.d.l.				20,00	b.d.l.	92,90	
E7	769430	305020	72,90	13,20	0,05	1,08	0,020	0,04	0,14	0,82	10,65	0,07	0,010	b.d.l.	0,030	99,01	0,33	2,06	1,67	b.d.l.	240,00	b.d.l.				15,30	b.d.l.	23,30	
E8	769720	304030	72,40	12,70	0,06	2,28	0,054	0,18	0,48	1,52	8,75	0,33	0,008	0,009		98,77		3,48	2,12			1,14				12,80	0,26	58,80	
E9	769380	304720	74,40	12,00	0,06	0,96	0,013	0,11	0,69	1,10	10,10	b.d.l.	0,006	0,003		99,43		1,22	1,25			1,89				11,90	0,50	29,90	
E10	769399	304736	72,44	13,71	0,06	1,37	0,010	0,11	0,12	0,97	10,59	0,05			0,002	99,43	0,60	b.d.l.	2,00	b.d.l.		1,00	b.d.l.			12,20			
E11	769708	304338	75,30	14,45	0,04	1,28	0,040	0,37	0,30	3,21	4,04	0,15		b.d.l.	b.d.l.	99,18	1,73			b.d.l.	10,00					18,80			
E12	769370	304123	72,86	14,67	0,05	1,65	0,03	0,30	0,35	3,55	4,90	0,23			b.d.l.	98,59	1,30	5,00	3,00	b.d.l.		0,70	b.d.l.			20,70			
E13	768589	305345	79,67	11,62	0,03	0,87	b.d.l.	0,16	0,68	6,13	0,07	0,11			b.d.l.	99,34	0,60	2,00	2,00	b.d.l.		0,40	b.d.l.			11,30			
E14	769647	304257	75,11	13,62	0,04	1,50	0,040	0,27	0,25	3,18	4,52	0,18			b.d.l.	98,71	1,30	1,00	3,00	b.d.l.		0,50	b.d.l.			19,90			
E15	769394	303935	79,45	11,34	0,03	1,42	0,040	0,34	0,33	2,87	2,62	0,23			b.d.l.	98,67	1,30	4,00	3,00	b.d.l.		0,30	b.d.l.			16,30			
E16	769272	304742	66,50	18,30	0,05	2,78	0,040	1,41	0,20	1,49	6,17	0,13			b.d.l.	97,07	2,90	8,00	4,00	b.d.l.		0,60	b.d.l.			27,70			
E17	769272	304742	49,08	27,12	0,12	5,65	0,070	1,94	0,25	0,05	10,59	0,19			b.d.l.	95,06	4,90	19,00	14,00	b.d.l.		0,60	b.d.l.			106,80			
E18	769280	304726	77,28	12,26	0,04	0,97	0,020	0,07	0,10	1,20	7,38	0,09			b.d.l.	99,41	0,60	6,00	2,00	b.d.l.		0,30	b.d.l.			16,50			
E19[c]	769837	304540	77,31	11,94	0,04	1,24	0,020	0,20	1,30	4,35	1,93	0,34			b.d.l.	98,67	1,30	5,00	3,00	b.d.l.		0,50	b.d.l.			12,50			
E20[c]	769131	304096	77,69	12,15	0,04	1,01	0,010	0,07	0,23	0,63	7,18	0,20			b.d.l.	99,21	0,80	2,00	3,00	b.d.l.		0,40	b.d.l.			18,00			
E21[c]	769165	304218	76,16	13,15	0,04	1,32	0,010	0,15	0,19	0,98	6,67	0,14			b.d.l.	98,81	1,20	3,00	3,00	b.d.l.		0,40	b.d.l.			17,90			
E22[c]	769165	304218	56,76	24,32	0,06	2,03	0,010	0,58	0,05	0,67	12,73	b.d.l.			b.d.l.	97,21	2,70	9,00	4,00	b.d.l.		0,40	b.d.l.			33,70			
E23	768230	305110	76,87	12,27	0,03	1,58	0,030	0,31	0,11	1,68	5,80	0,07			b.d.l.	98,75	1,30	3,00	2,00	10,00		0,70	b.d.l.			13,90			
E24	764710	306960	73,08	14,65	0,06	1,73	0,010	0,51	0,28	3,82	4,27	0,15			b.d.l.	98,56	1,40	2,00	4,00	b.d.l.		0,90	b.d.l.			20,70			
Szinva Metabasalt																													
F1	763570	307040	53,20	18,20	1,15	8,21	0,132	5,03	1,96	5,48	2,23	0,50	0,066	0,036		96,20		1,22	9,62			25,30				13,90	0,72	6,70	
F2	763050	307100	49,04	17,50	1,66	8,68	0,150	4,98	7,28	4,19	1,96	0,56			0,017	96,02	3,40	b.d.l.	17,00	148,00		23,50	64,00			14,10			
F3	762714	310604	47,15	17,51	1,55	9,53	0,130	10,18	0,95	5,40	1,00	0,49			0,026	93,92	5,80	2,00	16,00	115,00		31,70	143,00			14,60			
F4	761290	309873	46,86	18,27	1,35	9,37	0,140	9,78	1,79	5,12	0,98	0,51			0,022	94,19	5,50	3,00	16,00	139,00		28,70	102,00			13,40			
F5	769985	300558	47,70	17,80	2,12	6,77	0,123	7,74	4,27	2,15	3,85	0,42	0,071	0,044		93,05		1,30	17,00			38,70				15,90	0,73	17,90	
F6	770745	300928	48,00	14,90	1,69	9,70	0,076	11,70	0,70	2,60	3,06	0,34	0,006	0,002		92,78		1,23	18,60			38,10				12,10	0,71	11,40	
F7	770945	300940	47,39	17,03	1,88	9,56	0,120	12,27	0,77	1,01	1,65	0,39			0,031	92,10	7,60	1,00	24,00	178,00		39,30	203,00			15,40			
F8	771265	300748	50,00	19,00	2,11	12,10	0,028	4,19	0,24	0,06	6,39	b.d.l.	0,026	0,001		94,14		1,56	20,60			40,70				15,10	0,79	11,00	
F9	768850	303635	45,25	17,62	2,42	11,16	0,120	8,91	2,59	2,68	2,63	0,18			0,045	93,61	6,10	b.d.l.	35,00	281,00		36,80	120,00			19,50			
F10	767720	304990	43,19	22,10	2,46	14,65	0,020	2,91	0,25	0,07	9,69	0,12			0,063	95,52	4,30	3,00	37,00	166,00		49,70	152,00			18,90			
F11	766610	304715	47,06	16,98	1,24	8,63	0,140	9,12	6,34	2,44	2,99	0,20			0,042	95,18	4,50	b.d.l.	25,00	198,00		33,50	128,00			13,80			
F12	766830	305165	43,75	15,74	1,54	8,80	0,170	6,99	10,63	3,25	1,98	0,22			0,038	93,11	6,60	2,00	26,00	195,00		39,20	152,00			13,40			
F13	766685	305070	45,18	16,41	1,72	9,71	0,140	9,82	7,56	3,14	1,15	0,25			0,037	95,12	4,60	b.d.l.	27,00	226,00		29,50	136,00			13,50			
F14	766665	305410	46,90	17,95	1,80	8,85	0,110	8,73	3,39	3,41	2,71	0,38		0,020	0,012	94,26	5,02			273,00	110,00					19,80			
F15	761070	298450	41,60	13,40	1,70	10,04	0,132	8,96	5,95	1,68	3,32	0,22	0,048	0,020		87,07		1,08	19,00	253,00		36,70	43,50	34,30	117,00			2,08	
F16	760680	298760	47,40	15,30	2,60	7,73	0,128	4,95	2,22	2,33	3,80	0,25	0,063	0,015		86,79		1,03	31,30	386,00		51,70	42,60	165,00	108,00			22,60	
F17	760850	298490	45,60	13,60	2,10	7,06	0,096	7,23	6,24	2,47	3,65	0,39	0,049	0,014		88,50		b.d.l.	21,20	283,00		39,50	39,70	41,10	102,00			2,28	
F18	754910	304660	45,55	15,99	1,67	9,47	0,170	6,49	8,22	2,40	3,98	0,35			0,029	94,32	5,40	2,00	17,00	146,00		33,60	85,00			12,40			
F19	753749	291343	43,60	17,10	1,79	7,87	0,090	5,56	6,81	3,01	3,16	0,22			0,022	89,23	10,50	1,00	23,00	209,00		41,00	68,00			18,00			
Other samples																													
D3	751177	302757	53,27	17,23	1,92	8,75	0,070	7,77	0,58	5,53	0,05	0,29			0,050	95,51	4,20	b.d.l.	37,00	256,00		52,40	159,00			16,50			
G1	759490	305700	34,39	24,53	0,76	4,08	0,010	3,83	11,25	0,59	5,94	0,14			0,006	85,53	14,30	b.d.l.	6,00	95,00		11,40	25,00			15,10			
G2	757460	296320	41,45	15,61	0,96	10,21	0,180	5,22	9,55	5,29	0,29	0,21			0,073	89,04	10,80	2,00	22,00	126,00		41,60	143,00			15,00			
Control analyses																													
H1	767346	307898	61,95	17,24	0,98	3,90	0,06	0,92	3,39	3,05	3,56	0,17	0,02	0,02	0,013	95,27	4,60			91,00						19,00			
H2	767329	307622	60,37	17,91	1,21	5,48	0,06	2,49	2,40	2,83	2,19	0,14	0,02	0,02	0,009	95,13	4,70			79,00						18,10			
H3	767329	307622	67,59	11,62	0,95	6,82	0,07	3,68	2,12	1,20	0,97	0,23	0,01	0,01	0,003	95,27	4,60			50,00						12,70			
H4	755617	306154	67,13	15,05	0,82	5,66	0,03	0,43	0,38	3,16	5,53	0,22	0,02	0,01	0,002	98,44	1,40			49,00						20,40			
H5	755479	305920	68,56	14,41	0,44	5,08	0,02	0,39	0,56	3,65	5,47	0,07	0,02	0,01	0,003	98,68	1,20			22,00						20,30			
H6	769150	303958	76,31	12,47	0,04	1,22	0,01	0,06	0,04	0,68	8,11	0,05	b.d.l.	0,01	b.d.l.	99,00	1,00			b.d.l.						16,00			

sample id	Rb	Sr	Y	Zr	Nb	Sn	Sb	Cs	Ba	La	Ce	Pr	Nd	Sm	Eu	Gd	Tb	Dy	Ho	Er	Tm	Yb	Lu	Hf	Ta	W	Tl	Th	U
	ppm	ppm	ppm	ppm	ppm	ppm	ppm	ppm	ppm	ppm	ppm	ppm	ppm	ppm	ppm	ppm	ppm	ppm	ppm	ppm	ppm	ppm	ppm	ppm	ppm	ppm	ppm	ppm	ppm
Detection	0,25		0,25	0,25	0,25	0,50	0,10	0,25		0,25	0,25	0,10	0,10	0,10	0,05	0,10	0,10	0,10	0,10	0,10	0,10	0,10	0,10		0,25	0,25	0,10	0,25	0,25
Detection	0,20	0,10	0,10	2,00	0,20	1,00		0,01	0,50	0,10	0,10	0,03	0,10	0,03	0,03	0,05	0,01	0,05	0,01	0,03	0,01	0,03	0,01	0,20	0,10	1,00		0,05	0,05
Detection	0,10	0,50	0,10	0,10	0,10	1,00		0,10	1,00	0,10	0,10	0,02	0,30	0,05	0,02	0,05	0,01	0,05	0,02	0,03	0,01	0,05	0,01	0,10	0,10	0,50		0,20	0,10
Detection	10,00			10,00					10,00																				
Bagolyhegy Metarhyolite																													
E1	354,00		17,90	41,50	13,90	22,60	0,31	33,30		4,55	11,30	1,48	5,83	2,14	0,06	2,16	0,59	3,52	0,62	1,47	0,21	1,28	0,18	2,35	2,63	3,32	1,79	6,53	11,00
E2	408,90	22,90	19,30	35,30	10,30	22,00		32,60	12,00	3,60	8,20	1,06	3,70	1,73	0,03	2,17	0,59	3,84	0,61	1,55	0,22	1,43	0,18	1,80	2,00			5,70	6,80
E3	277,00		15,70	35,90	10,10	17,10	0,40	24,90		3,32	8,19	1,10	4,03	1,61	0,06	1,65	0,48	2,92	0,52	1,35	0,20	1,16	0,14	1,51	1,77	12,10	1,56	5,01	5,91
E4	205,00		10,40	52,00	10,20	15,00		16,30		5,09	7,99	1,14	4,15	1,51	0,05	1,40	0,38	2,09	0,38	0,98	0,15	0,93	0,13		1,70	3,75	1,80		3,55
E5	132,00		11,80	51,00	10,30	7,85		8,88		10,60	11,50	1,28	4,01	1,48	0,06	1,42	0,37	2,38	0,43	1,12	0,16	0,98	0,13		2,12	10,00	1,05	4,67	2,94
E6	406,00	37,80	7,70	35,00	9,50	17,00		19,10	19,10	3,00	5,80	0,79	3,20	1,02	0,05	1,18	0,26	1,46	0,22	0,61	0,06	0,51	0,07	1,30	1,80	5,00	2,37	4,46	6,23
E7	452,00	54,00	8,90	47,00	9,60	12,00		21,90	52,80	4,60	8,00	1,06	3,30	1,03	b.d.l.	1,21	0,26	1,76	0,28	0,74	0,07	0,62	0,06	1,70	1,90	6,00	3,00	5,18	7,92
E8	311,00		18,30	53,00	9,85	16,00		16,70		7,82	14,00	1,73	6,08	2,34	0,10	2,33	0,62	3,58	0,63	1,59	0,23	1,33	0,19		1,82	7,01	2,52		8,42
E9	325,00		6,19	56,00	9,46	13,60		19,20		5,61	7,78	1,03	3,81	1,01	0,10	0,80	0,20	1,11	0,22	0,64	0,10	0,65	0,10		1,63	1,81	1,67	5,00	5,67
E10	388,10	21,50	7,00	38,70	9,80	17,00		20,30	33,00	1,90	4,50	0,56	2,20	0,86	0,02	1,02	0,23	1,36	0,21	0,54	0,08	0,56	0,07	1,90	1,80	1,20		5,80	6,90
E11	288,00		8,10	36,00	10,30	23,00		22,40	13,00	2,20	5,00	0,70	2,60	1,11	0,04	1,20	0,30	1,65	0,26	0,63	0,10	0,78	0,09	1,90	1,90	6,00		4,48	3,16
E12	373,30	23,40	14,60	45,70	14,00	24,00		29,30	10,00	3,30	7,30	0,87	3,40	1,26	0,02	1,61	0,45	2,72	0,43	1,19	0,16	1,18	0,14	2,20	2,30			6,40	4,70
E13	5,90	240,50	10,80	33,50	10,10	15,00		0,60	4,00	3,50	7,80	0,96	3,60	1,35	0,02	1,67	0,38	2,27	0,36	0,81	0,11	0,63	0,08	1,70	1,60	1,30		5,50	7,20
E14	347,50	12,90	11,00	40,50	11,20	23,00		25,30	6,00	3,20	6,30	0,88	2,90	1,15	b.d.l.	1,38	0,35	2,08	0,33	0,83	0,14	0,91	0,12	2,00	2,10	1,70		6,10	3,90
E15	247,30	33,90	10,10	35,50	10,40	19,00		22,30	5,00	3,30	7,90	0,83	2,80	1,13	b.d.l.	1,43	0,34	1,99	0,32	0,81	0,13	0,86	0,12	1,60	1,90	2,60		4,90	4,70
E16	703,80	14,10	14,40	48,30	16,60	28,00		69,30	5,00	3,90	7,10	0,89	2,80	1,13	b.d.l.	1,71	0,41	2,69	0,44	1,08	0,15	0,99	0,12	2,50	2,40	5,80		7,50	7,60
E17	>1000	3,90	19,90	112,90	25,80	149,00		71,00	7,00	3,60	10,20	1,49	5,70	2,44	b.d.l.	2,93	0,71	4,15	0,64	1,74	0,26	1,81	0,24	5,80	1,20	4,50		17,50	32,90
E18	384,40	35,70	7,80	37,50	10,10	17,00		18,40	8,00	2,70	5,10	0,58	2,00	0,68	b.d.l.	0,79	0,20	1,33	0,23	0,62	0,09	0,70	0,09	2,00	1,90	3,70		5,70	7,50
E19[c]	158,20	21,20	23,70	36,30	11,60	17,00		14,20	3,00	4,20	8,60	1,07	3,70	1,73	b.d.l.	2,57	0,71	4,32	0,68	1,67	0,21	1,35	0,16	1,90	1,90	2,40		5,00	15,60
E20[c]	363,80	56,10	23,60	32,30	10,70	17,00		16,00	12,00	4,20	9,40	1,22	4,60	2,40	b.d.l.	3,24	0,79	4,41	0,71	1,74	0,21	1,33	0,17	1,70	1,80	7,60		5,90	11,10
E21[c]	376,30	36,20	14,50	36,50	11,20	20,00		15,50	9,00	4,00	8,60	1,06	3,70	1,53	b.d.l.	1,82	0,44	2,60	0,43	1,10	0,16	1,05	0,14	1,90	2,00	3,80		5,90	22,90
E22[c]	728,10	30,50	17,90	60,60	17,40	42,00		30,00	17,00	6,40	13,00	1,37	3,70	0,96	b.d.l.	1,20	0,37	2,80	0,54	1,50	0,21	1,35	0,19	3,20	2,30	7,80		7,90	36,20
E23	281,80	50,00	4,70	27,10	8,70	13,00		16,50	33,00	1,20	1,70	0,32	1,00	0,43	b.d.l.	0,56	0,14	0,85	0,14	0,39	0,05	0,35	0,03	1,30	1,40	3,40		3,10	4,50
E24	261,70	43,90	13,00	44,60	12,20	22,00		20,80	14,00	3,50	7,30	1,09	4,00	1,55	0,05	1,88	0,44	2,62	0,40	1,05	0,14	0,94	0,12	2,10	2,20	3,20		6,50	4,20
Szinva Metabasalt																													
F1	54,00		17,50	105,00	44,10	1,71		1,33		29,90	50,60	5,86	21,80	4,47	1,55	4,40	0,68	3,55	0,70	1,91	0,29	1,86	0,30		2,55	2,75	1,27	4,73	0,18
F2	42,20	2070,10	26,80	186,60	65,10	1,00		1,00	1177,00	39,90	68,50	7,84	30,20	5,51	1,84	5,76	0,81	4,88	0,96	2,78	0,39	2,61	0,41	4,20	3,80	0,60		7,40	1,80
F3	24,80	63,10	24,20	180,70	64,90	1,00		1,90	61,00	48,10	80,70	8,96	32,50	5,56	1,71	5,06	0,76	4,28	0,92	2,59	0,39	2,64	0,42	4,10	3,80	1,40		6,40	1,20
F4	38,60	94,50	24,40	206,40	72,50	1,00		16,40	49,00	40,40	67,90	7,67	28,30	5,01	1,59	4,72	0,73	4,26	0,88	2,57	0,37	2,51	0,39	4,50	4,00	0,90		8,10	1,70
F5	56,70		24,30	184,00	48,90	4,64		7,92		30,60	50,40	6,12	24,00	5,25	1,68	4,78	0,82	4,76	0,96	2,74	0,40	2,47	0,38		3,09	0,97	1,34	4,49	0,18
F6	45,80		19,00	116,00	38,50	1,95		2,03		29,00	44,70	5,23	20,50	4,51	1,19	3,80	0,66	3,93	0,82	2,29	0,34	2,11	0,33		2,38	1,22	0,99	3,60	0,16
F7	27,50	16,00	27,80	146,60	42,10	1,00		1,60	102,00	38,20	66,10	8,02	31,30	6,26	2,06	6,19	0,96	5,48	1,11	3,09	0,45	2,91	0,40	3,50	2,50	0,80		4,20	1,00
F8	118,00		19,80	126,00	48,00	1,33		4,42		31,20	50,10	6,39	24,70	5,02	1,40	4,27	0,72	4,12	0,84	2,25	0,33	2,06	0,30		2,75	1,30	0,71	4,82	0,26
F9	45,30	95,00	24,70	170,30	32,90	1,00		1,20	174,00	17,00	42,20	5,77	24,20	5,16	1,98	5,27	0,80	4,64	0,95	2,82	0,39	2,44	0,36	4,00	2,00	b.d.l.		3,10	1,30
F10	129,50	7,00	33,60	222,30	39,70	2,00		4,80	250,00	28,90	61,50	7,58	29,80	6,27	1,98	6,73	1,08	6,57	1,35	3,68	0,53	3,34	0,51	5,50	2,10	b.d.l.		3,40	0,90
F11	41,20	312,20	20,50	95,00	18,10	b.d.l.		2,50	632,00	17,80	36,30	4,65	18,40	3,74	1,49	3,98	0,62	3,71	0,79	2,26	0,33	2,15	0,32	2,40	0,80	b.d.l.		1,70	0,60
F12	32,00	191,40	22,80	128,40	21,10	b.d.l.		0,60	221,00	15,30	31,40	4,17	18,00	4,12	1,32	4,54	0,73	4,16	0,89	2,47	0,34	2,13	0,33	3,10	1,20	b.d.l.		2,20	0,50
F13	19,50	266,70	25,60	144,60	25,30	1,00		0,50	202,00	14,80	32,60	4,45	19,40	4,56	1,37	5,02	0,80	4,85	1,02	2,83	0,40	2,54	0,37	3,30	1,50	b.d.l.		2,50	0,70
F14	33,40		34,50	156,00	33,30	3,00		0,61	558,00	29,90	63,00	7,89	32,90	6,35	2,43	6,86	1,04	6,52	1,20	3,66	0,53	3,56	0,54	3,60	1,20	9,00		3,16	1,07
F15	40,40		22,00	111,00	19,80	b.d.l.	0,27	3,33	465,00	10,50	22,30	3,17	13,90	3,65	1,27	3,70	0,68	4,25	0,89	2,49	0,36	2,29	0,35		1,24	2,49		2,71	b.d.l.
F16	61,90		31,00	147,00	24,20	b.d.l.	22,20	1,53	525,00	15,10	27,20	4,61	20,70	5,43	1,69	5,41	1,03	6,10	1,22	3,44	0,49	3,07	0,47		1,54	5,22		3,01	b.d.l.
F17	49,90		26,00	134,00	24,60	b.d.l.	16,20	1,77	398,00	15,60	31,30	4,17	18,30	4,61	1,54	4,78	0,83	5,11	1,08	3,05	0,45	2,84	0,43		1,63	5,76		3,35	b.d.l.
F18	68,70	154,50	28,20	172,40	30,70	2,00		7,20	401,00	18,80	40,30	5,26	22,10	4,88	1,52	5,30	0,82	5,00	0,98	2,88	0,41	2,64	0,40	3,80	1,80	b.d.l.		3,70	0,70
F19	42,30	253,60	25,60	138,30	27,20	2,00		2,10	284,00	19,60	34,80	4,12	17,30	3,77	1,19	4,37	0,70	4,37	0,91	2,51	0,36	2,42	0,36	3,40	1,70	b.d.l.		4,00	1,10
Other samples																													
D3	1,20	147,40	29,80	164,10	15,70	b.d.l.		0,40	89,00	8,30	18,20	2,58	12,10	3,23	1,07	4,18	0,74	5,12	1,09	3,37	0,50	3,22	0,51	4,00	1,00	b.d.l.		1,50	0,40
G1	114,80	93,70	9,30	205,30	20,10	12,00		23,20	227,00	30,00	62,90	3,49	9,90	1,53	0,20	1,50	0,27	1,84	0,45	1,31	0,22	1,50	0,24	8,80	2,30	2,50		50,10	0,40
G2	8,20	139,60	17,50	75,70	4,50	b.d.l.		0,40	30,00	8,80	17,50	2,53	11,90	3,01	0,85	3,59	0,53	3,38	0,66	1,89	0,26	1,72	0,25	2,10	0,30	b.d.l.		1,70	0,40
Control analyses																													
H1	142,60	132,20	34,50	249,20	11,00			10,20	394,00	36,40	63,80	8,36	33,50	7,00	1,18	6,57	1,07	6,37	1,21	3,50	0,51	3,12	0,48	6,60	0,90			11,50	2,60
H2	104,30	166,70	32,30	199,10	9,70			8,50	424,00	25,80	54,00	6,61	27,40	6,18	1,19	5,94	0,99	5,71	1,15	3,12	0,47	2,89	0,42	5,10	0,70			8,30	5,00
H3	42,30	63,40	35,80	180,20	8,30			3,20	204,00	22,60	46,90	6,05	25,20	5,55	0,89	5,78	1,00	6,32	1,23	3,63	0,52	3,40	0,51	4,70	0,70			7,60	15,80
H4	210,80	63,70	50,60	358,40	14,10			8,10	458,00	44,20	89,80	11,22	44,60	9,60	1,11	9,34	1,55	9,19	1,84	5,15	0,78	4,82	0,73	10,00	1,10			16,70	3,60
H5	185,10	93,30	42,80	357,60	12,00			4,70	451,00	38,60	79,60	9,54	36,40	7,57	0,96	7,33	1,22	7,78	1,52	4,47	0,69	4,73	0,73	9,10	0,90			14,70	3,30
H6	389,80	66,60	5,60	37,50	10,90			17,50	17,00	3,40	6,90	0,77	3,00	0,89	0,02	0,90	0,21	1,38	0,17	0,52	0,08	0,63	0,08	2,00	1,70			4,70	7,30

Table 1 (continued)

Colours indicate analyst and method: black – Hungarian Geological Institute (ICP), blue – ALS (ICP), green – Bureau Veritas (ICP), red – University of Miskolc (WDXRF). Missing numbers indicate that the element was not assayed in the sample; b.d.l. indicates elements below detection limit. Upper index c indicates drillcore samples: B2: Bszk-60, 39.5–40.0 m; E19: B-37, 155.3–155.8 m; E20: Bszk-2, 11.0–11.5 m; E21: B-13, 115.1–116.8 m; E22: B-13, 276.1–278.4 m

Table 2 Position of the additional samples used in mineralogical tests but not analysed for trace elements

Samples	X	Y
B30	306,140	767,210
B31	306,080	767,850
C11	298,100	763,715
E25	303,970	769,130
E26	304,100	769,110
F20	305,395	766,630
F21	298,450	761,040

Coordinates are given in the Hungarian National Projection System (EOV)

(CO_2 and water content mainly) is indicated by the LOI values. Quality assurance was made by the laboratories testing standards, blanks and duplicates in each measurement packages. 6 additional unpublished analyses from an earlier project used for testing the validity of our results are also included (control analyses in Table 1).

Mineralogical and petrographical properties were studied on 34 of the assayed samples, and additionally on further 7 samples taken from the same rock bodies which were not assayed, in the University of Miskolc, Institute of Mineralogy and Geology. Coordinates of the sampling sites not included in Table 1 are shown in Table 2. Samples were chosen to represent major geochemical groups and special textures. We used a Zeiss Axio Imager A2m (polarized light, transmission and reflection mode, APO objectives, AxioCam MRc 5 camera) microscope for thin sections. X-ray powder diffraction of bulk samples was made by a Bruker D8 Advance diffractometer (Cu-Kα radiation, parallel beam geometry with Göbel mirror, accelerating voltage 40 kV, tube current 40 mA, Våntec-1 position sensitive detector). For primary phase evaluation DiffracPlus EVA software was used, with components identification by Search/Match on ICDD PDF4-2018 database. We accepted those matches only, which were supported also by observations made with other methods. Quantitative evaluation was made by Rietveld refinement in TOPAS4 software, instrumental profile determined on NIST SRM 640a Si. Amorphous content was calculated through fitting the amorphous hump with a Pawley peak combined with Rietveld refinement. In case of minerals with overlapping peaks on the XRD pattern we also considered EDX composition data of the minerals of the same samples. A JEOL JXA-8600 Superprobe electron microprobe (20 kV accelerating voltage, 20 nA probe current, carbon coating) was used for observations on backscattered electron images and standardless (semi-quantitative) EDX point and area measurements on polished sections. Element distributions were investigated by X-ray mapping (EDX map) in qualitative mode, with baseline correction and counting times ranging from 10 to 20 min per frame.

Geological setting of the metavolcanics

The Bükk Mts. (NE Hungary) is an uplifted part of the Pre-Cenozoic basement of the Pannonian Basin on the NW side of the Mid-Hungarian Fault Zone. Except minor remnants of the Paleogene and Neogene sedimentary and volcanic rocks, the Bükk exposes successions ranging from Upper Carboniferous to Middle Jurassic. Stratigraphy was established and mapped by Balogh (1964) and, following significant revisions, by Less et al. (2005), but still retaining formations of ambiguous identity. These successions were correlated with several localities of the Dinarides and the Southern Alps (Balogh 1964; Kovács et al. 2000), implying hundreds of kilometres tectonic displacement since the primary rock-forming processes.

The Paraautochthonous Unit is derived from continental crust (Balogh 1964; Harangi et al. 1996; Less et al. 2005) in three successions (Upper Carboniferous, Upper Permian–Upper Triassic and Middle Jurassic), of which the Permian–Triassic one contains metavolcanics only (Fig. 1). These rocks suffered Cretaceous ductile deformation and coeval regional metamorphism (Árkai 1973, 1983; Árkai et al. 1995) to various degrees. The synmetamorphic fold axes are gently W-SW-plunging in general. Most intensive deformation and dynamic recrystallization of the limestone (Németh and Mádai 2005) was observed in the central part of the Bükk Mts, while well preserved fossils were retrieved from outcrops of the same formations at the NW and S edges (Balogh 1964; Less et al. 2005).

The differences in deformation style of this synmetamorphic phase are most easily observed in the folding style of sedimentary formations comprising alternating limestone and chert or siliciclastic beds. Based on these and minor stratigraphic differences, four major structural units representing tectofacies units can be delineated. According to the typical E–W or SE–NW strike of the boundary faults in the eastern part of the Mts, we refer to these as Northwestern Bükk, Northeastern Bükk, Central Bükk and Southeastern Bükk Unit (Fig. 1) in the followings. Three of these

contain Triassic metavolcanics: Northeastern Bükk (NU), Central Bükk (CU) and Southeastern Bükk Unit (SU). The boundaries are mainly steep or vertical strike-slip faults dissected by later faults and thrusts at several segments, but there is no direct evidence of the original fault sense. Small (100–1000 m)-scale fault blocks of alternating stratigraphic content are typical in the boundary zones. NU also includes an imbricated thrust unit named Kis-fennsík Nappe, but rocks of the thrust blocks (including metavolcanics) still belong to the tectofacies of the NU.

There were four metavolcanic formations mapped (Less et al. 2005): Szentistvánhegy Metaandesite, Bagolyhegy Metarhyolite, Szinva Metabasalt and Létrás Metabasalt, named according to the textural observations and SiO_2 content range of the assayed samples (summarized in Balogh 1964). However, the definition of these formations is not applicable at all outcrops because distinguishing criteria used for mapping were mostly the contacts with over- and underlying formations. Two of the occurrences have paleontologically dated sedimentary successions: both under- and overlying limestone are Ladinian in the Szentistvánhegy horizon, and the limestone embedding a Szinva Metabasalt body at Felsőtárkány is Carnian (site F19 in Fig. 1), dated by Conodonts (Less et al. 2005). At other outcrops, including the large Bükkszentlászló block, the contacted formations may differ from these, and may be either undated or not successive. Because of that, the stratigraphic position of the metavolcanic bodies remains ambiguous and has been variably indicated on published geological maps in several cases. The detailed description of the stratigraphic position of the metavolcanics and the stratigraphic consequences of our results are given in Appendix A. Figure 1 shows the position of the outcrops coloured according to a revised stratigraphic division.

Geochemical characterization and revision of the metavolcanics stratigraphic units

Parameters used for characterization

The database established by new sampling and assaying of the metavolcanics bodies (Table 1) provides the basis for a revised more reliable stratigraphic division. The major element composition of the sampled rocks varies in wide intervals. The calcium content is typically very low except in peperitic rocks with calcite. For most of the samples from each unit, alkaline metals are present in higher concentration than in a typical calc-alkaline volcanic suite. Potassium and sodium are in several cases enriched at the expense of each other, which can be interpreted as a signature of alteration. Based on major element geochemistry, we cannot identify the original magmatic character of the rocks.

Trace element composition also shows anomalies which are unlikely to be of magmatic origin. Recent studies revealed that even trace elements regarded commonly as immobile are involved in geochemical anomalies (Németh et al. 2016). Accordingly, samples containing a high field strength elements (HFSE) enrichment hosted partly by metavolcanics (i.e. samples taken from rock bodies where $\Sigma REE > 500$ ppm and $Zr > 1000$ ppm were confirmed) were filtered out from the database, but some of the remaining ones (e.g. samples C4 and C7 from the vicinity of HFSE-enriched bodies) may be still affected by the mobilizing processes. Despite this, different HFSE distributions are characteristic for certain groups of metavolcanic bodies. Proportions of elements behaving similarly in post-magmatic

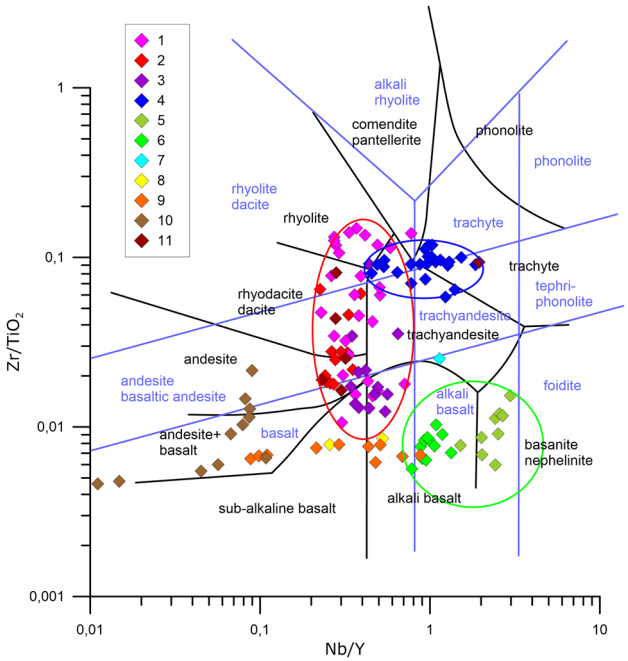

Fig. 2 Trace element-based classification diagram for altered metavolcanics proposed by Winchester and Floyd (1977). Fields redefined by Pearce (1996) are shown in blue lines and rock names, original ones in black. Colour codes for the plotted data points (data in Table 4, locations in Fig. 1): 1 – SMV Szentistvánhegy horizon and Kis-fennsík area, NU (samples A1–A12); 2 – SMV Bükkszentlászló block, NU (samples B1–B28); 3 – SMV Miklós-luga area and SW Bükk, SU and boundary of CU and Szarvaskő nappe in the W (samples C1–C11, D1–D2); 4 – BMR (samples E1–E24); 5 – SMB NE group (samples F1–F8); 6 – SMB SW group (samples F9–F19); 7 – pseudotachylite from SMV Bükkszentlászló block (sample B29); 8 – other samples (samples D3, G1–2); 9 – Darnó/Hosszúvölgy Metabasalt (data published by Kiss et al. 2016); 10 – Szarvaskő Metabasalt (data published by Kiss et al. 2016); 11 – control analyses (H1–H6). Ellipses outline the characteristic distribution intervals for the formations BMR (blue), SMV (red) and SMB (green)

processes were found to have remained fairly constant. These bodies can be defined as genetically related, either as volcanic products of the same magmatism or as products of the same subsequent metasomatic alteration. Some samples belonging to the metavolcanics formations of recognized or supposed non-magmatic origin (redeposited volcaniclastic material, tectonites, metavolcanics penetrated by veins) were also included in the database. The aim of this is to demonstrate how these transformation processes of the metavolcanics influence their geochemical composition.

Winchester and Floyd (1977) proposed a classification of metavolcanics based on the concentration ratios Zr/TiO_2 indicating the original grade of differentiation and Nb/Y indicating the original alkalinity. This diagram was applied instead of the TAS diagram for altered rocks to reveal the original volcanic rock types, using stable trace elements.

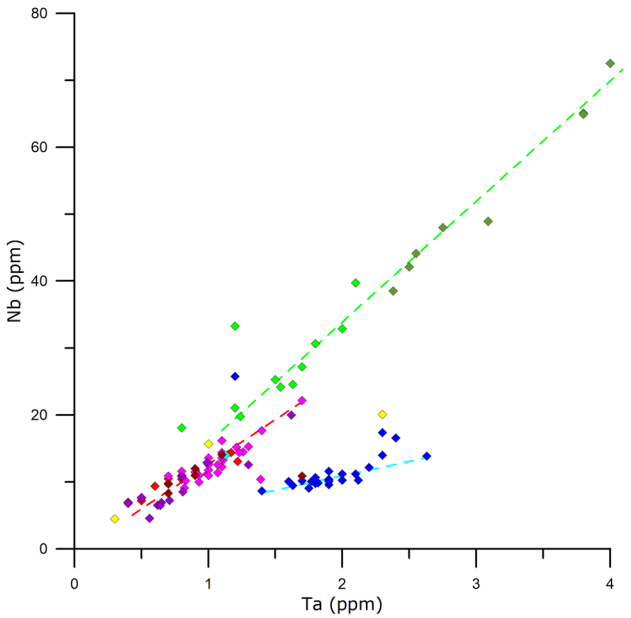

Fig. 3 Niobium and tantalum concentration data (Table 1) with calculated linear regression functions for three groups. Colour codes for the plotted data points are the same as in Fig. 2. Regressions: red – SMV; cyan – BMR; green – SMB

Data of our assayed samples are plotted in Fig. 2, for comparison together with published analyses from the metavolcanics of the Szarvaskő Unit (Kiss et al. 2016). Our data form three distinct groups marked by ellipses, also clearly distinguished from the metavolcanics of the Szarvaskő Unit. The relationship of Nb and Ta concentrations (Fig. 3) was plotted as a further property which, in combination with the Zr/TiO_2 vs. Nb/Y diagram, proved to be distinctive for the magma source. Statistical parameters of these ratios are summarized in Table 3; all calculated values are shown in Table 4. REE distribution patterns, extended with other assayed HFSE, also proved to be useful, supporting the geochemical grouping (Fig. 4). Tetrad effects were quantified using the indices based on relative standard deviations proposed by Monecke et al. (2002). Although Eu was mobilized in different processes than other REE, Eu anomalies (Table 4) in most of the samples still were found to be related to the magmatic composition. Ta/Yb and Th/Yb ratios were used after Pearce (1982) to decide whether the magma originated from a subduction zone of a volcanic arc or from a mantle source of within-plate or middle-oceanic ridge setting (Fig. 5).

According to these data, three large clusters of the samples are delineated. These clusters are suitable for discriminating the formations Bagolyhegy Metarhyolite (BMR), Szentistvánhegy Metavolcanics (SMV) and Szinva Metabasalt (SMB), corresponding to the three marked groups in Fig. 2. These names will be used in the followings as reinterpreted names of valid stratigraphic units. The former "metaandesite" in the case of the SMV was modified to metavolcanics because of the variable rock types. Outliers and other special samples appearing on the diagrams also will be discussed. The Y or Nb anomaly in three of the samples, linked to alteration, caused significant change in the parameter values Nb/Y and Nb/Ta (Tables 3, 4.). Using other properties these samples could be also assigned to the appropriate formation.

Parameters calculated from control analyses of samples from certain stratigraphic position matched perfectly to the expected groups (Figs. 2, 3 and 5): H1–H5 represent the Szentistvánhegy horizon of SMV in outcrops not sampled in this study; H6 represents the type locality of BMR.

Table 3 Geochemical parameters used for identification of metavolcanics formations (*Calculated omitting the Nb-enriched samples E17 and E22; **Calculated omitting the Y-depleted sample B29)

	Bagolyhegy metarhyolite (24 samples)			Szentistvánhegy metavolcanics (54 samples)			Szinva metabasalt (19 samples)		
	Zr/TiO_2	Nb/Y*	Nb/Ta*	Zr/TiO_2	Nb/Y**	Nb/Ta	Zr/TiO_2	Nb/Y	Nb/Ta
Median	0.091	0.970	5.51	0.028	0.363	12.56	0.008	1.182	16.96
Range	0.054	1.398	2.06	0.138	0.551	10.02	0.010	2.191	7.53
Variance	0.014	0.360	0.49	0.042	0.122	2.09	0.002	0.735	1.66
Var/med	0.15	0.37	0.09	1.50	0.34	0.17	0.25	0.62	0.10

Table 4 Calculated significant geochemical parameters for the assayed samples

	Szentistvánhegy Metavolcanics												
sample id	A1	A2	A3	A4	A5	A6	A7	A8	A9	A10	A11	A12	B1
Y	759070	759080	759105	759110	759120	759160	759225	759270	759280	760390	760697	762047	764406
X	307490	307540	307570	307600	307640	307690	307710	307730	307750	311980	312369	310969	306839
Zr/TiO_2	0,065	0,025	0,028	0,027	0,028	0,018	0,020	0,018	0,018	0,022	0,046	0,061	0,060
Nb/Y	0,225	0,278	0,264	0,327	0,299	0,246	0,241	0,259	0,271	0,353	0,332	0,392	0,359
Nb/Ta	14,00	15,00	13,00	14,50	15,67	14,40	15,20	17,00	17,50	13,75	10,74	12,31	11,77
Th/Yb	3,02	2,75	2,80	2,60	2,81	2,21	2,09	2,08	2,30	4,20	3,18	2,89	4,47
Ta/Yb	0,16	0,19	0,22	0,20	0,19	0,18	0,16	0,15	0,17	0,33	0,26	0,29	0,31
REE	193,32	169,44	170,32	149,08	131,89	119,03	112,12	103,56	96,31	154,22	208,10	176,01	265,22
Ce/Ce*	1,00	0,93	0,97	1,04	1,03	0,94	0,99	1,00	1,00	0,97	0,98	0,72	0,81
Eu/Eu*	0,39	0,48	0,52	0,49	0,56	0,63	0,68	0,66	0,75	0,54	0,43	0,53	0,33
HREE/MREE	0,80	0,69	0,72	0,81	0,79	0,74	0,80	0,77	0,77	0,58	0,91	0,89	0,64
HREE/LREE	0,25	0,23	0,22	0,27	0,27	0,27	0,33	0,30	0,29	0,17	0,24	0,22	0,15
T_1	0,02	0,05	0,02	0,04	0,02	0,04	0,01	0,02	0,04	0,02	0,05	0,19	0,26
T_3	0,04	0,02	0,03	0,03	0,04	0,08	0,04	0,06	0,03	0,03	0,05	0,06	0,02
T_4	0,01	0,05	0,02	0,08	0,07	0,04	0,05	0,02	0,07	0,06	0,04	0,03	0,05

sample id	B2	B3	B4	B5	B6	B7	B8	B9	B10	B11	B12	B13	B14
Y	764107	766650	766626	769915	769760	769420	769460	769660	769660	769850	769860	768830	768495
X	307141	306410	306559	305125	305320	305700	305700	305540	305600	304970	306298	306330	305897
Zr/TiO_2	0,026	0,118	0,016	0,114	0,132	0,136	0,011	0,032	0,042	0,078	0,060	0,067	0,118
Nb/Y	0,333	0,279	0,492	0,583	0,273	0,414	0,303	0,319	0,459	0,392	0,509	0,504	0,490
Nb/Ta	15,57	12,80	12,56	12,29	11,51	7,48	11,13	11,18	10,75	11,31	11,83	11,80	11,78
Th/Yb	4,08	4,63	3,56	3,98	Th n.a.	Th n.a.	Th n.a.	3,54	Th n.a.	4,17	4,73	5,02	3,70
Ta/Yb	0,21	0,20	0,37	0,28	0,20	0,40	0,28	0,39	0,33	0,27	0,34	0,32	0,30
REE	128,16	168,53	206,75	61,73	251,41	138,21	122,40	197,96	95,89	143,72	107,86	173,28	80,94
Ce/Ce*	1,03	0,84	0,93	0,93	0,97	0,95	0,84	0,92	0,82	0,96	0,98	0,96	0,87
Eu/Eu*	0,77	0,16	0,74	0,91	0,30	0,45	0,65	0,51	0,83	0,45	0,40	0,55	0,59
HREE/MREE	0,71	1,08	0,67	2,54	0,91	1,26	0,71	0,71	1,15	0,93	1,06	0,90	1,36
HREE/LREE	0,28	0,30	0,16	0,49	0,27	0,26	0,25	0,19	0,30	0,26	0,27	0,18	0,48
T_1	0,02	0,11	0,05	0,07	0,04	0,06	0,11	0,05	0,17	0,03	0,03	0,04	0,09
T_3	0,06	0,02	0,06	0,14	0,03	0,04	0,04	0,05	0,05	0,07	0,01	0,05	0,10
T_4	0,10	0,05	0,04	0,07	0,06	0,04	0,02	0,10	0,05	0,02	0,02	0,03	0,03

sample id	B15	B16	B17	B18	B19	B20	B21	B22	B23	B24	B25	B26	B27
Y	769530	769435	769475	769980	769133	767850	768589	769366	769760	768149,6	770060	768886	769185
X	304845	305040	305280	305248	305655	306080	305345	304935	305320	304974,4	305175	305835	306025
Zr/TiO_2	0,078	0,125	0,148	0,018	0,139	0,020	0,015	0,034	0,106	0,019	0,140	0,016	0,047
Nb/Y	0,263	0,273	0,370	0,711	0,776	0,308	0,461	0,273	0,292	0,431	0,335	0,364	0,229
Nb/Ta	12,78	10,65	11,71	11,98	13,06	13,09	13,60	12,82	12,64	14,50	12,60	11,00	14,73
Th/Yb	3,21	3,64	3,69	5,00	4,41	3,36	4,86	3,65	4,69	3,75	4,16	2,57	2,20
Ta/Yb	0,20	0,26	0,24	0,51	0,33	0,25	0,41	0,25	0,27	0,30	0,22	0,32	0,14
REE	215,73	197,01	153,97	145,63	93,78	209,66	220,75	228,11	261,95	139,76	156,35	145,94	291,82
Ce/Ce*	0,85	0,89	0,83	0,97	1,00	0,90	1,02	0,95	0,98	0,97	0,89	1,03	0,91
Eu/Eu*	0,41	0,34	0,45	2,18	0,26	0,53	0,71	0,50	0,33	0,67	0,20	0,62	0,25
HREE/MREE	0,72	0,79	1,11	0,71	2,53	0,73	0,54	0,73	0,64	0,74	0,92	0,72	0,74
HREE/LREE	0,21	0,22	0,34	0,16	0,63	0,22	0,12	0,21	0,21	0,20	0,30	0,24	0,30
T_1	0,10	0,07	0,12	0,04	0,07	0,07	0,03	0,03	0,04	0,02	0,07	0,03	0,07
T_3	0,06	0,09	0,10	0,05	0,09	0,02	0,03	0,04	0,01	0,02	0,04	0,04	0,04
T_4	0,04	0,04	0,02	0,04	0,04	0,06	0,04	0,07	0,06	0,08	0,01	0,05	0,05

sample id	B28	B29	C1	C2	C3	C4	C5	C6	C7	C8	C9	C10	C11
Y	771590	771510	765965	765145	764890	764290	764120	764080	763460	762730	762730	762160	753362
X	306560	306460	297679	297819	297870	298040	297830	297840	297830	297875	297875	297840	291228
Zr/TiO_2	0,045	0,025	0,012	0,016	0,013	0,034	0,017	0,021	0,022	0,016	0,017	0,091	0,035
Nb/Y	0,381	1,138	0,545	0,476	0,438	0,348	0,343	0,380	0,419	0,562	0,493	0,438	0,647
Nb/Ta	12,36	12,39	10,57	10,69	10,53	12,35	8,20	10,16	13,03	10,21	17,25	9,69	13,86
Th/Yb	4,03	4,73	2,89	2,66	2,97	3,05	2,83	2,65	3,61	3,26	4,84	8,96	5,85
Ta/Yb	0,27	0,51	0,44	0,30	0,33	0,24	0,34	0,34	0,32	0,37	0,32	0,38	0,59
REE	133,01	18,04	79,69	64,87	79,35	254,05	89,41	91,89	167,91	68,37	81,29	162,51	101,19
Ce/Ce*	0,95	0,82	0,94	1,22	1,24	0,95	1,00	0,99	0,96	0,86	0,92	1,40	0,89
Eu/Eu*	0,33	2,90	0,88	0,90	0,72	0,37	0,91	0,65	0,45	0,73	0,89	0,45	0,55
HREE/MREE	0,88	2,71	0,85	1,36	0,87	0,96	0,80	0,71	0,71	1,30	0,77	1,01	0,48
HREE/LREE	0,34	1,88	0,25	0,42	0,29	0,29	0,20	0,23	0,20	0,28	0,16	0,26	0,11
T_1	0,04	0,19	0,04	0,16	0,22	0,04	0,04	0,06	0,04	0,09	0,05	0,32	0,08
T_3	0,01	0,12	0,04	0,02	0,01	0,02	0,01	0,04	0,03	0,01	0,05	0,02	0,06
T_4	0,09	0,07	0,03	0,04	0,02	0,03	0,03	0,02	0,04	0,02	0,07	0,03	0,07

Table 4 (continued)

	SMV		Bagolyhegy Metarhyolite										
sample id	D1	D2	E1	E2	E3	E4	E5	E6	E7	E8	E9	E10	E11
Y	749746	750545	769530	769530	769540	769620	769310	769360	769430	769720	769380	769399	769708
X	301968	302487	304480	304470	304530	304070	304100	305180	305020	304030	304720	304736	304338
Zr/TiO_2	0,013	0,014	0,070	0,088	0,082	0,118	0,091	0,058	0,094	0,096	0,100	0,065	0,090
Nb/Y	0,382	0,363	0,777	0,534	0,643	0,981	0,873	1,234	1,079	0,538	1,528	1,400	1,272
Nb/Ta	13,50	15,40	5,29	5,15	5,71	6,00	4,86	5,20	5,05	5,41	5,80	5,44	5,42
Th/Yb	3,31	3,01	5,10	3,99	4,32	Th n.a.	4,77	8,75	8,35	Th n.a.	7,69	10,36	5,74
Ta/Yb	0,27	0,24	2,05	1,40	1,53	1,83	2,16	3,53	3,06	1,37	2,51	3,21	2,44
REE	138,79	88,29	35,39	28,91	26,73	26,37	35,92	18,23	22,99	42,57	23,16	14,11	16,66
Ce/Ce*	0,98	0,96	1,04	1,01	1,03	0,80	0,75	0,90	0,87	0,91	0,78	1,05	0,97
Eu/Eu*	0,64	0,69	0,08	0,05	0,11	0,10	0,13	0,14	0,04	0,13	0,34	0,06	0,11
HREE/MREE	0,71	0,61	0,57	0,59	0,63	0,66	0,66	0,44	0,45	0,58	0,87	0,56	0,60
HREE/LREE	0,22	0,26	0,49	0,71	0,60	0,40	0,26	0,30	0,24	0,39	0,28	0,50	0,55
T_1	0,04	0,03	0,12	0,14	0,16	0,14	0,20	0,06	0,13	0,06	0,17	0,09	0,12
T_3	0,02	0,02	0,40	0,46	0,44	0,39	0,34	0,35	0,30	0,38	0,28	0,35	0,41
T_4	0,05	0,04	0,01	0,06	0,10	0,04	0,03	0,20	0,24	0,03	0,02	0,10	0,19

sample id	E12	E13	E14	E15	E16	E17	E18	E19	E20	E21	E22	E23	E24
Y	769370	768589	769647	769394	769272	769272	769280	769836,6	769130,9	769165	769165	768230	764710
X	304123	305345	304257	303935	304742	304742	304726	304539,7	304096,1	304218,2	304218,2	305110	306960
Zr/TiO_2	0,091	0,112	0,101	0,118	0,097	0,094	0,094	0,091	0,081	0,091	0,101	0,090	0,074
Nb/Y	0,959	0,935	1,018	1,030	1,153	1,296	1,295	0,489	0,453	0,772	0,972	1,851	0,938
Nb/Ta	6,09	6,31	5,33	5,47	6,92	21,50	5,32	6,11	5,94	5,60	7,57	6,21	5,55
Th/Yb	5,42	8,73	6,70	5,70	7,58	9,67	8,14	3,70	4,44	5,62	5,85	8,86	6,91
Ta/Yb	1,95	2,54	2,31	2,21	2,42	0,66	2,71	1,41	1,35	1,90	1,70	4,00	2,34
REE	24,03	23,54	20,57	21,96	23,41	35,91	15,11	30,97	34,42	26,63	33,59	7,16	25,08
Ce/Ce*	1,03	1,02	0,90	1,14	0,91	1,06	0,98	0,97	1,00	1,00	1,05	0,66	0,90
Eu/Eu*	0,04	0,04	0,02	0,02	0,02	0,01	0,04	0,01	0,01	0,02	0,03	0,06	0,09
HREE/MREE	0,62	0,41	0,65	0,63	0,55	0,62	0,78	0,47	0,42	0,59	0,89	0,53	0,51
HREE/LREE	0,63	0,35	0,55	0,53	0,53	0,71	0,52	0,62	0,57	0,51	0,49	0,50	0,46
T_1	0,06	0,08	0,14	0,19	0,11	0,21	0,05	0,10	0,09	0,11	0,22	0,25	0,12
T_3	0,49	0,33	0,41	0,36	0,35	0,40	0,35	0,48	0,38	0,35	0,41	0,37	0,38
T_4	0,11	0,03	0,12	0,06	0,08	0,06	0,10	0,06	0,06	0,04	0,02	0,28	0,05

	Szinva Metabasalt												
sample id	F1	F2	F3	F4	F5	F6	F7	F8	F9	F10	F11	F12	F13
Y	763570	763050	762714	761290	769985	770745	770945	771265	768850	767720	766610	766830	766685
X	307040	307100	310604	309873	300558	300928	300940	300748	303635	304990	304715	305165	305070
Zr/TiO_2	0,009	0,011	0,012	0,015	0,009	0,007	0,008	0,006	0,007	0,009	0,008	0,008	0,008
Nb/Y	2,520	2,429	2,682	2,971	2,012	2,026	1,514	2,424	1,332	1,182	0,883	0,925	0,988
Nb/Ta	17,29	17,13	17,08	18,13	15,83	16,18	16,84	17,45	16,45	18,90	22,63	17,58	16,87
Th/Yb	2,54	2,84	2,42	3,23	1,82	1,71	1,44	2,34	1,27	1,02	0,79	1,03	0,98
Ta/Yb	1,37	1,46	1,44	1,59	1,25	1,13	0,86	1,33	0,82	0,63	0,37	0,56	0,59
REE	127,87	172,39	194,59	167,30	135,36	119,41	172,53	133,70	113,98	159,82	96,54	89,90	95,01
Ce/Ce*	0,92	0,93	0,93	0,92	0,88	0,87	0,91	0,85	1,02	1,00	0,96	0,94	0,96
Eu/Eu*	1,06	0,99	0,98	0,99	1,02	0,87	1,00	0,92	1,15	0,93	1,17	0,93	0,87
HREE/MREE	0,64	0,68	0,77	0,76	0,71	0,76	0,66	0,66	0,68	0,70	0,76	0,68	0,70
HREE/LREE	0,15	0,15	0,13	0,15	0,19	0,18	0,16	0,15	0,24	0,23	0,24	0,27	0,30
T_1	0,06	0,07	0,05	0,06	0,10	0,13	0,08	0,11	0,08	0,04	0,03	0,04	0,02
T_3	0,03	0,07	0,07	0,04	0,03	0,02	0,03	0,02	0,04	0,02	0,05	0,04	0,03
T_4	0,05	0,06	0,04	0,05	0,04	0,04	0,02	0,01	0,04	0,04	0,02	0,07	0,02

							Other samples		
sample id	F14	F15	F16	F17	F18	F19	D3	G1	G2
Y	766665	761070	760680	760850	754910	753749	751177	759490	757460
X	305410	298450	298760	298490	304660	291343	302757	305700	296320
Zr/TiO_2	0,009	0,007	0,006	0,006	0,010	0,008	0,009	0,027	0,008
Nb/Y	0,965	0,900	0,781	0,946	1,089	1,063	0,527	2,161	0,257
Nb/Ta	27,75	15,97	15,71	15,09	17,06	16,00	15,70	8,74	15,00
Th/Yb	0,89	1,18	0,98	1,18	1,40	1,65	0,47	33,40	0,99
Ta/Yb	0,34	0,54	0,50	0,57	0,68	0,70	0,31	1,53	0,17
REE	166,38	69,80	95,96	94,09	111,29	96,78	64,21	115,35	56,87
Ce/Ce*	0,98	0,93	0,78	0,93	0,97	0,93	0,94	1,25	0,88
Eu/Eu*	1,12	1,05	0,95	1,00	0,91	0,89	0,88	0,40	0,78
HREE/MREE	0,73	0,79	0,72	0,79	0,71	0,75	0,98	1,25	0,68
HREE/LREE	0,23	0,39	0,36	0,35	0,26	0,27	0,67	0,15	0,34
T_1	0,01	0,05	0,15	0,06	0,02	0,09	0,05	0,33	0,10
T_3	0,05	0,04	0,09	0,01	0,03	0,03	0,04	0,04	0,06
T_4	0,03	0,04	0,05	0,03	0,04	0,03	0,04	0,03	0,04

Table 4 (continued)

Formulae: $Ce^* = \sqrt{(La^*Pr)}$; $Eu^* = \sqrt{(Sm^*Gd)}$; $HREE = Tm_{C1} + Yb_{C1} + Lu_{C1}$; $MREE = Gd_{C1} + Tb_{C1} + Dy_{C1}$; $LREE = La_{C1} + Pr_{C1} + Nd_{C1}$; $T_i = \sqrt{\frac{1}{2} \times \left[\left(\frac{x_{Bi}}{x_{Ai}^{2/3} \times x_{Di}^{1/3}} - 1 \right)^2 + \left(\frac{x_{Ci}}{x_{Ai}^{1/3} \times x_{Di}^{2/3}} - 1 \right)^2 \right]}$, where x_{Ai}, x_{Bi}, x_{Ci} and x_{Di} are C1 normalized concentrations of REE in the i-th tetrad. According to Monecke et al (2002), T_i values exceeding 0.2 indicate tetrad effect safely beyond analytical errors, but T_1 values influenced by Ce anomaly are not meaningful

Geochemical characteristics of the Bagolyhegy Metarhyolite

This formation is characterized by ~ 0.1 (0.065–0.120) Zr/TiO_2, ~ 6 Nb/Ta and variable, but generally high Nb/Y ratios (0.4–1.9) (Fig. 2.). The rocks of the BMR are rich in K, Cs, Rb and U, but depleted in Ba, Sr and HFSE (Fig. 4). The depletion of REE is more pronounced in the case of the light REEs (median of HREE/LREE is 0.5; of HREE/MREE is 0.59) and particularly strong in the case of Eu (median of Eu/Eu* is 0.063). A significant M-type tetrad effect ($T_3 = 0.28–0.49$, Table 4) was found in the third tetrad only. The parameters indicate felsic rocks formed from highly differentiated, silica-saturated magma of within-plate character (mantle originated in Fig. 5).

Potassium and rubidium enrichment are widespread (samples E6–E10, E16–E18, E20–E22), mainly in samples representing silicified and pyritic rock bodies (samples E6–E10). Additionally, samples E17 and E22 are depleted in SiO_2 and show positive anomaly of Al, Fe, Ti and several trace elements, including Zr, Nb but not Ta. This causes significant shift in the Nb/Ta ratio, while Zr and TiO_2 remained correlated. Sample E23 is extremely REE and Y depleted, with a negative Ce anomaly, resulting the highest Nb/Y ratio in this cluster. Sample E13 is Na and Sr enriched and strongly K, Rb and Cs depleted, taken from the contact with SMV

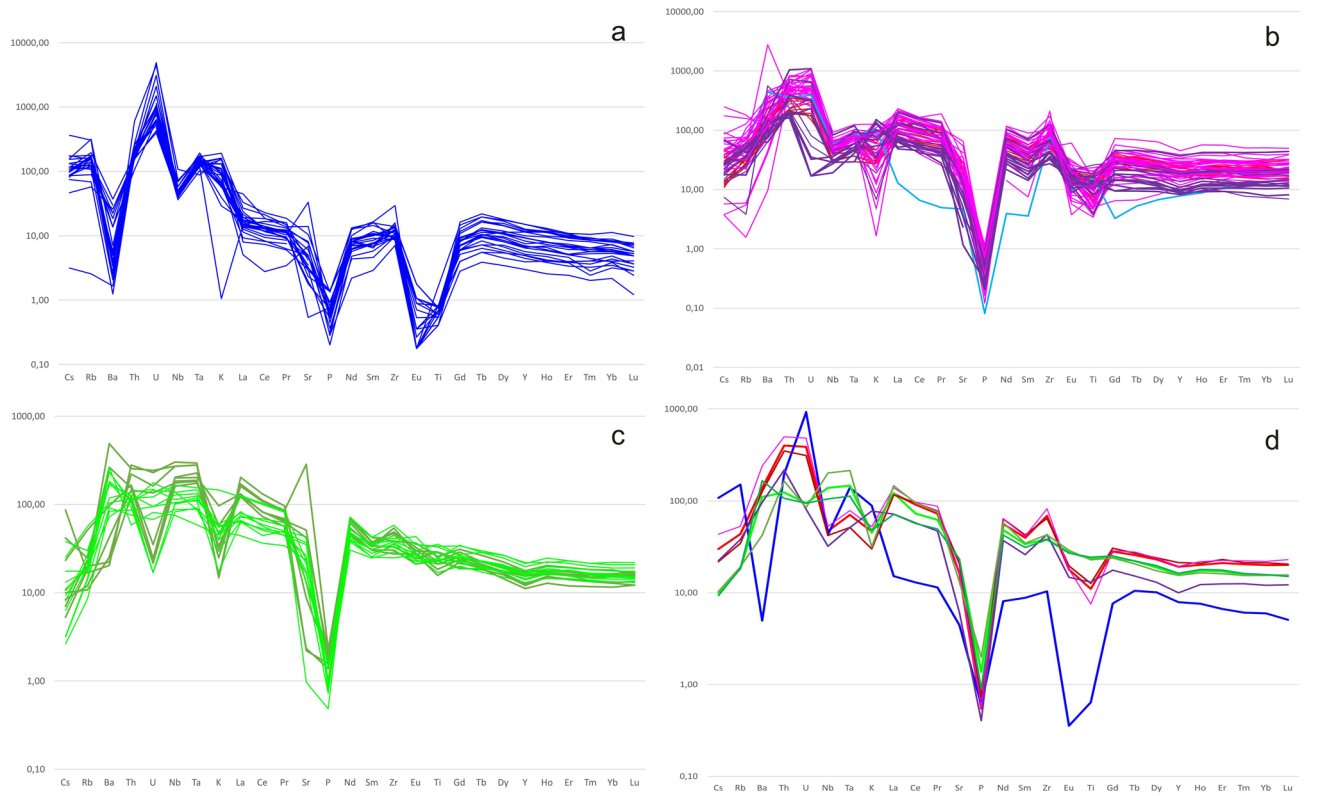

Fig. 4 Spider diagrams of C1 chondrite (McDonough and Sun 1995) normalized trace element concentrations of the assayed metavolcanic samples (Table 1). Concentrations below or beyond detection limit were left out. Colour codes for the plotted data are the same as in Fig. 2. **a** BMR; **b** SMV; **c** SMB; **d** median values for each formation (bold lines) and subgroups (thin lines)

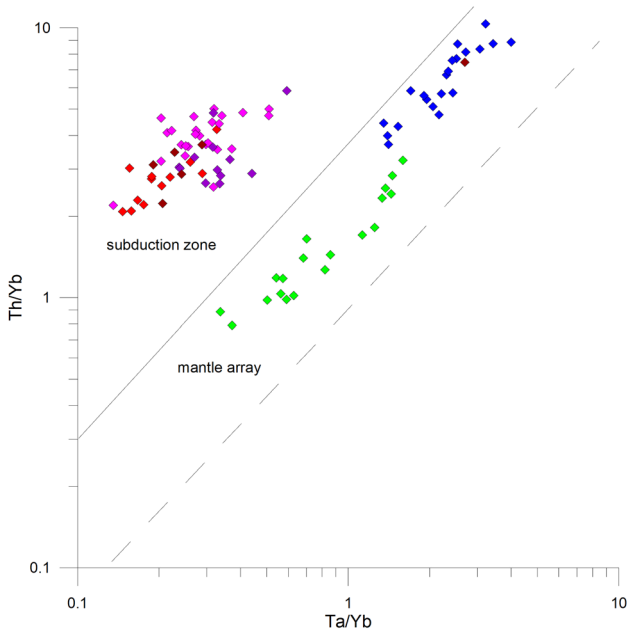

Fig. 5 Discrimination diagram for island arc and mantle originated magmatic rocks after Pearce (1982). Th and Ta are used as stable trace element proxies for K and Si, respectively, Yb as a normalizing factor. Plotted Th/Yb and Ta/Yb values are given in Table 4. Samples with lacking Th concentration data and with significant Th anomalies (Table 1) were omitted. Colour codes for the plotted data are the same as in Fig. 2

represented by sample B21, which is, on the contrary, K enriched. Sample E1 shows relatively high Be, U and REE concentration as it is the country rock of an apatite layer hosting more significant enrichment of these elements (Zajzon et al. 2014).

Geochemical characteristics of the Szentistvánhegy Metavolcanics

This formation is much more voluminous; therefore, more samples were needed than for the BMR and SMB. Also, a territorial subdivision was carried out, indicated by the letters A-D in the sample identifiers (A: Szentistvánhegy horizon and Kis-fennsík area of the NU, B: Bükkszentlászló block of the NU, C: SU occurrences, D: Bélapátfalva area, blocks at the boundary of Szarvaskő nappe and CU). The SMV is characterized by a wide range of Zr/TiO_2 ratios between 0.01 and 0.15, Nb/Y ratios between 0.2 and 0.8 but typically lower than 0.4 (Fig. 2.), and ~ 13 Nb/Ta ratio. REE patterns show Eu depletion increasing with the higher grade of differentiation; Eu/Eu* is correlated with Zr/TiO_2, mainly at lower values of the latter ratio. Plots in Fig. 5 indicate island arc character. The formation represents a calc-alkaline volcanic suite.

Variability of the Zr/TiO_2 ratios (Table 3 and Fig. 2) was characteristic within an outcrop and within the subgroups as well, related to the grade of differentiation. Samples A1–A9 represent a continuous section of the complete SMV from top to bottom in the Szentistvánhegy horizon; in most other sites of this horizon the formation is truncated by faults. Here 0.018–0.020 Zr/TiO_2 ratios were typical in the lower and 0.025–0.027 in the upper half of the section, which can be interpreted as an underlying less differentiated andesitic and an overlying more differentiated andesitic or dacitic member, reflecting the magma evolution.

In the Kis-fennsík area (samples A10–A12) and in the large Bükkszentlászló block (samples B1–B29) Zr/TiO_2 ratios are generally higher than values of samples A1–A9, in several cases exceeding 0.1. Lower ratios were obtained mostly in samples taken from rock bodies with amygdaloidal texture (samples B4, B20, B26). On the other hand, more than half of the samples of the Miklós-luga (SU, samples C1–C10) area, the sample of Felsőtárkány (C11) and two samples of the Bélapátfalva area (samples D1–D2) have low 0.012–0.020 Zr/TiO_2 ratios. Here the REE contents are generally lower except Eu. These variations indicate that different outcrop areas represent suites of separate volcanic centres.

Potassium and Rb enrichment together with low Na concentrations is widespread in the Miklós-luga area (samples C1–C3, C5, C7–C10) and present in the Bükkszentlászló block as well (samples B2, B3, B19, B21, B23). In some cases of silicified rocks, both K and Na concentrations are rather high (samples B5–B7, B11, B13, B25). In sample B2, additional boron metasomatism (1770 ppm B) is accompanied by some Ti depletion, raising the Zr/TiO_2 value. Sample C1 was taken at a peperitic contact, hence the excess calcium. Samples B1, B12 and B20 represent Na-enriched and K-depleted rocks, B5 and B14 are depleted in light REEs and Y, causing high Eu/Eu* values, while B18 contains positive Ba and Eu anomalies. Sample B19 is Nb and Zr enriched. Sample B27, taken at the contact with limestone, is enriched in REE (except Eu) and Y. Sample B29 represents pseudotachylite, a special fault rock within the metavolcanics with prominent Y and REE depletion except Eu; this anomaly significantly shifts the Nb/Y ratio but not the Zr/TiO_2 and the Nb/Ta ratios. Samples C4 and C7 may be affected by the HFSE enrichment found in nearby rock bodies; sample C7 contains positive anomalies in all HFSE, causing a high Zr/TiO_2 ratio. Sample C11 is depleted in heavy REEs and Y.

Geochemical characteristics of the Szinva Metabasalt

This formation is characterized by low < 0.01 Zr/TiO_2 ratios and generally high, but variable Nb/Y ratios (0.7–3.0)

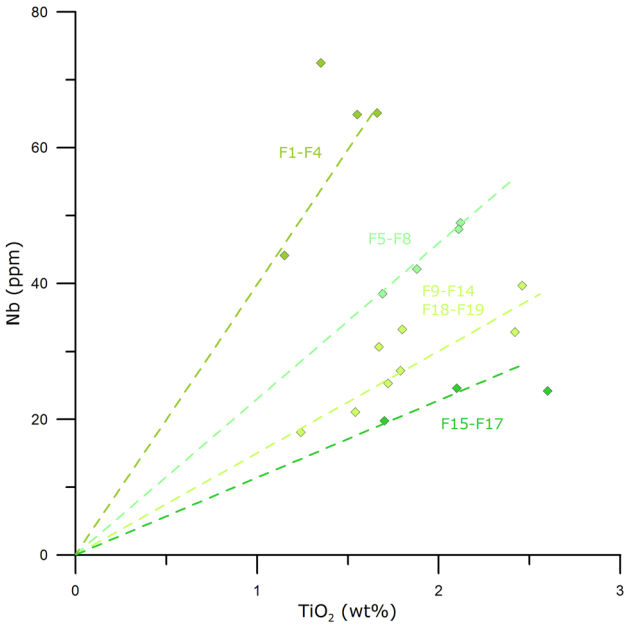

Fig. 6 Niobium and titanium oxide concentration data of the samples F1–F19 (Table 1) representing the Szinva Metabasalt. Dashed lines indicate the ratios typical for the subgroups symbolized with different shades of green

(Fig. 2), and the Nb/Ta ratio is ~ 17. Eu, Nb, Ta and Ti concentrations are higher, and other trace element concentrations are lower than in the SMV in general (Fig. 4). But when compared to the SMV samples with similarly low Zr/TiO_2 ratios (basaltic rocks) only, most trace element concentrations are higher in SMB. Actual concentration values are also influenced by the amount of calcite in peperitic samples, as concentrations of most trace elements are expected to be low in the lime mud-derived part of the rocks. The calculated ratios indicate alkaline basaltic rocks of within-plate character (mantle originated in Fig. 5) in this formation.

There is also a tendency of spatial variability in compositions observed. According to that, two major geographical groups can be defined: the Northeastern (samples F1–F8 from the NU and eastern part of the CU) and the Southwestern (samples F9–F19 from the CU and the SU). They can be divided by the 1.4 Nb/Y ratio value, with the NE group displaying higher and the SW group displaying lower values. NE group samples tend to contain more SiO_2, light REE, P, Nb, Ta and Th than samples of the SW group. These variations may indicate different magmatic sources for the two groups. If we assume that Nb and Ti were dominantly contained by Ti-Fe oxide minerals in the magmatic paragenesis of these rocks, and these elements were not mobilized in metasomatic alterations (except the filtered out HFSE enrichment); then Nb vs TiO_2 distribution reflects the original composition of the magma and can also be used for refinement of the clustering (Fig. 6). NU samples (F1–F4) yielded the highest Nb/Ti ratios, followed by the eastern CU samples of the NE group (F5–F8), while all SW group ratios are lower; the lowest values were obtained for samples representing the Hór Valley outcrops (F15–F17).

Geochemical anomalies were found in sample F2 enriched in Ba and Sr, in samples F8 and F10 enriched in K and Rb, while F10 and F14 are enriched in Nb, Y and heavy REE.

Mineralogical and petrographic characteristics of the metavolcanics stratigraphic units

General textural properties of the metavolcanics

Photomicrographs referred to in the followings and description of the methods followed by identification of the minerals are shown in Appendix B.

To recognize the texture of the studied rocks as of volcanic origin is not always clear and straightforward. The common characteristic feature is the textural inhomogeneity in grain size and mineral composition as well, in contrast with most of the sedimentary or metasedimentary rocks of the same successions. Typical crystal grains of the matrix are smaller than 10 µm. Porphyroclasts or pseudomorphs of phenocrystals in the 0.1–3 mm range, or lithoclasts even up to some centimetres are often recognizable, although distorted in sheared and dynamically recrystallized textures (Figure B1a), and brecciated rocks also occur (Figure B2a). Relict porphyroclasts are altered and partly replaced in several cases. Minerals which can be interpreted as of magmatic origin are abundant in few basaltic samples only (e.g., idiomorphic, fractured and partly altered clinopyroxene, Figure B3a), in several cases absent completely.

Contacts in the NU and CU are usually strongly sheared, and so is the texture of several rocks. Effusive, intrusive, pyroclastic, or redeposited characteristics are in several cases obliterated by synmetamorphic ductile deformation but are retained in the tectofacies of the SU. Similarly, these characteristics can have been retained in other units as well if a competent rock body (e.g., a silicified body; welded rocks; a body created by a lava flow or intrusion) was embedded in incompetent matrix (e.g., fine-grained or argillitized pyroclastics or sediments). Such features can be typical volcanic texture patterns (e.g. peperitic, Figure B2a or intersertal, Figure B3b), flow lamination with disharmonic folds restricted to distinct layers (Figure B1b), or the occurrence of enclosed lithoclasts or altered vitroclasts (Figure B2c).

The texture often contains layers or lenses of varying composition and competence at various scales also

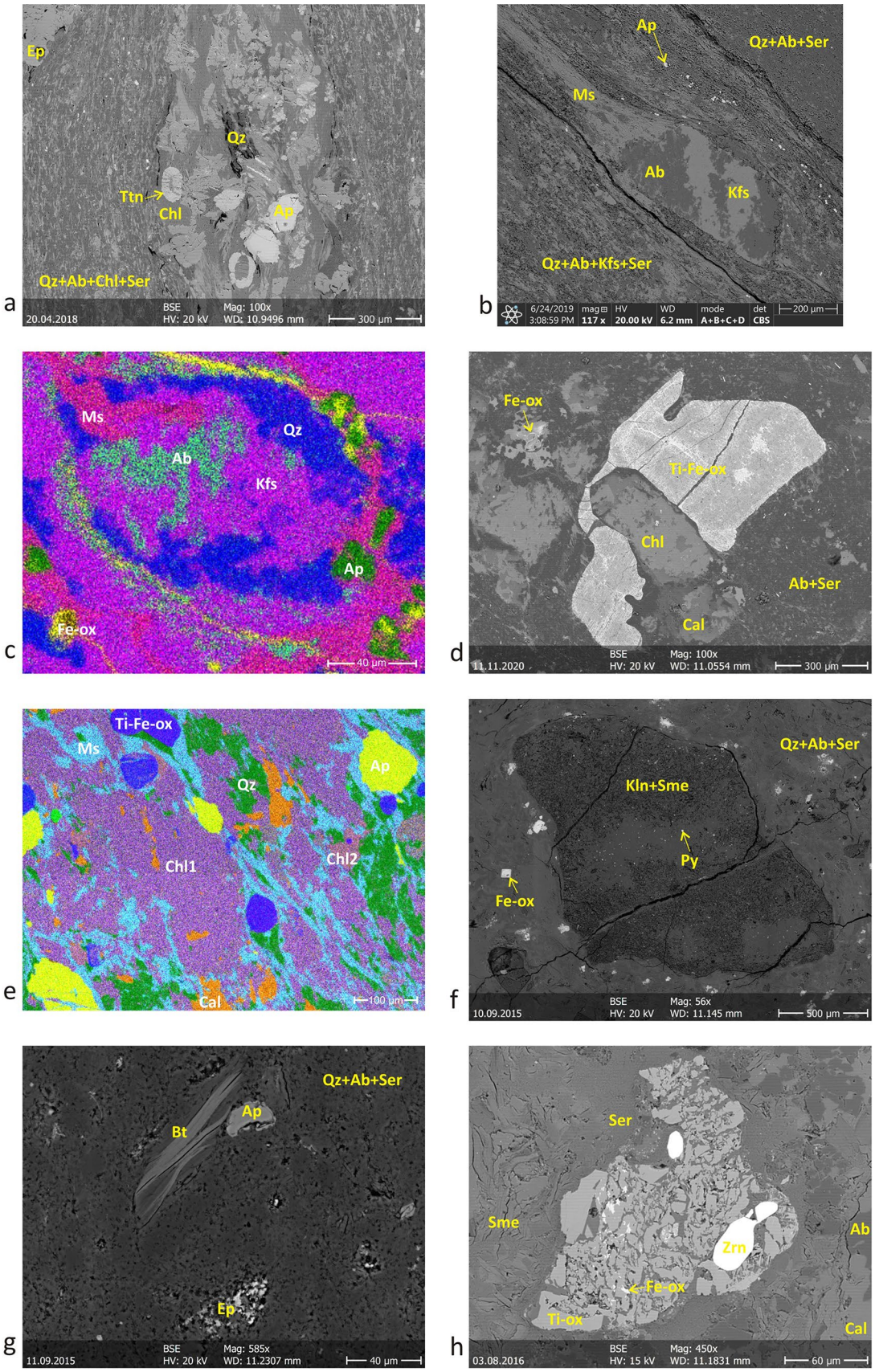
a
Ep
Qz
Ttn
Chl
Ap
Qz+Ab+Chl+Ser
20.04.2018
BSE
HV: 20 kV
Mag: 100x
WD: 10.9496 mm
300 µm
b
Ap
Qz+Ab+Ser
Ms
Ab
Kfs
Qz+Ab+Kfs+Ser
6/24/2019
3:08:59 PM
mag
117 x
HV
20.00 kV
WD
6.2 mm
mode
A+B+C+D
det
CBS
200 µm
c
Ms
Qz
Ab
Kfs
Ap
Fe-ox
40 µm
d
Fe-ox
Ti-Fe-ox
Chl
Ab+Ser
Cal
11.11.2020
BSE
HV: 20 kV
Mag: 100x
WD: 11.0554 mm
300 µm
e
Ti-Fe-ox
Ms
Qz
Ap
Chl1
Chl2
Cal
100 µm
f
Qz+Ab+Ser
Kln+Sme
Py
Fe-ox
10.09.2015
BSE
HV: 20 kV
Mag: 56x
WD: 11.145 mm
500 µm
g
Qz+Ab+Ser
Ap
Bt
Ep
11.09.2015
BSE
HV: 20 kV
Mag: 585x
WD: 11.2307 mm
40 µm
h
Ser
Sme
Ab
Zrn
Fe-ox
Ti-ox
Cal
03.08.2016
BSE
HV: 15 kV
Mag: 450x
WD: 11.1831 mm
60 µm

◂**Fig. 7** Backscattered electron images. Mineral abbreviations: Ab – albite, Ap – apatite, Bt – biotite, Cal – calcite, Ep – epidote, Kfs – K-feldspar, Kln – kaolinite, Ms – muscovite (phengite), Py – pyrite, Qz – quartz, Ser – sericite, Sme – smectite, Ttn – titanite, Ti-Fe-ox – titanium-iron oxide minerals. **a** A layer of epidote, titanite, apatite, fine-grained sericite and chlorite in quartz-albite-chlorite-sericite matrix. Bright spots and stripes in epidote are REE enriched. Sample B30, Lillafüred, Kerek Hill quarry, SMV Bükkszentlászló block (NU). **b** Relict albite with resorbed edges, partly replaced by potassic feldspar in an oriented quartz-feldspar-sericite matrix with apatite fragments. Sample E11, Hidegvíz Valley, BMR (NU). **c** Coloured EDX element map of a replaced porphyry feldspar. Sample E6, Hidegvíz Valley, BMR (NU). **d** Relict ilmenite with exsolution lamellae of hematite. The ilmenite has an inhomogeneous composition indicating incomplete alteration to titanite and hematite. The enclosed idiomorphic grain (probably pyroxene) is completely altered to clinochlore, calcite and muscovite. Sample A3, Vadász Valley, SMV Szentistvánhegy horizon (NU). **e** Coloured EDX element map of relict ilmenite and apatite grains in clinochlore and phengite-dominated matrix, with more and less Fe-rich chlorite types. Sample A3, Vadász Valley, SMV Szentistvánhegy horizon (NU). **f** Plagioclase pseudomorph replaced by smectite and kaolinite, with disseminated pyrite and iron oxide after pyrite in quartz-sericite matrix with iron oxide pseudomorphs after pyrite. Sample C4, Miklós-luga, SMV Miklós-luga area (SU). **g** Biotite with Fe-Ti content varying across the lamellae, apatite and REE-containing epidote in quartz-sericite matrix. Sample C10, Hidegpatak Valley, SMV Miklós-luga area (SU). **h** Fractured anatase associated with rounded zircon grains in peperite. Fractures are filled with calcite and Fe-oxides. The matrix is dominated by smectites and calcite. Sample from the same site as C1, Pap-Hárs Hill, SMV Miklós-luga area (SU)

in cases where a fabric is developed (Fig. 7a). The competent lenses are flattened parallel with the cleavage enveloping them like the porphyroclasts, resulting in an anastomosing pattern. Thin competent layers may display small-scale folding (Figure B1c, d). Cleavage is defined by the shape preferred orientation (SPO) of the fine grains of the matrix, particularly if the proportion of phyllosilicates is relatively high. Sericite or chlorite may be concentrated in cleavage domains (Figure B3c) or in strain shadows at porphyroclasts (Figure B3d). Abundance of such domains tends to cause exfoliation of the rocks. Macroscopic intensity of the cleavage, therefore, depends not on the amount of strain primarily but on the proportion of phyllosilicates in the composition.

In ductile shear zones the metavolcanics are mylonitized, which can be observed mainly at the contacts of rock bodies, both within and at the boundaries of the formations. The fringes of the often broken and dissected porphyroclasts are asymmetric, indicating rotation (Fig. 7b), and shear band cleavage is developed (Figure B2d), or the cleavage is folded (Figure B3e). Pseudotachylite (sample B29) was also found, where folded sericitic clasts of the metavolcanics with albite phenocrystals dissected into subgrains are embedded in a dark, glassy matrix (Figure B2e, f).

Mineralogical and petrographic characteristics of the Bagolyhegy Metarhyolite

The rocks of this formation consist almost entirely of felsic minerals (Group 1 in Fig. 8). Quartz and microcline add up to ca. 3/4 of the mineral composition in most cases. Orthoclase, albite, and phengitic muscovite or illite ($2M_1$ polytype) are the further rock-forming minerals in variable proportions. Common accessories are pyrite (or iron minerals after pyrite), rutile, ilmenite, biotite (annite), fluorapatite and zircon, but their abundance is low, and any of these may be missing. Amorphous (glassy) material content is typically low, except for two samples taken from the same silicified lens. Heating experiments on samples from the same formation showed the crystallization of orthoclase and microcline at the expense of amorphous material and quartz accompanied by water loss (Tóth and Kristály 2017).

The fine-grained matrix contains ca. 1/10 of mm-scaled porphyroclasts (quartz or albite phenocrystals, or aggregates as pseudomorphs after feldspars or, occasionally, after mafic minerals), overgrown by sericitic strain fringes and envelopes. The matrix comprises quartz and potassic feldspars with sericite seams and lenses. Quartz phenocrystals have rounded, resorbed edges (Figure B1e) and undulating extinction. Albites are angular and fragmented, often replaced partly by K-feldspars (Figure B1a, Fig. 7b). Some rocks display compositional layering (Figure B1b, c) or contain lenses which differ from the matrix (Figure B1d, f).

White or light grey quartz or quartz-albite veins are common, both following and dissecting the cleavage, and both with undeformed idiomorphic and with altered and deformed phenocrystals reaching cm-scale size in some cases. Mineral occurrences of tourmaline, rutile, and HFSE-oxides (Fehér 2015; Gál et al. 2022) are bound to such veins, but the majority of these contain quartz and albite only.

There is a typical rock type of the BMR which is often exposed. It forms lenses of some tens of metres in thickness elevated as small natural cliffs from the less resistant country rocks. Erosion of these cliffs produces also abundant blocky and splintery debris on the slopes and in the valleys with metre-scale blocks. Fresh rocks are massive, and their colour is grey because they contain fine-grained pyrite dissemination. Weathered rocks are brownish or reddish because of the oxidation of the pyrite. These rocks are dominated by potassic feldspars (> 50% of the mineral composition). The strain of these lenses was of flattening type, without rotational shear markers in the fabric. Even sericitic microlenses (Figure B1f) are not transposed into cleavage domains like in most other cases, where shear markers can be observed (Figure B1g). The competence contrast of these bodies and their country rocks indicates silicification and potassium metasomatism preceding the synmetamorphic deformation.

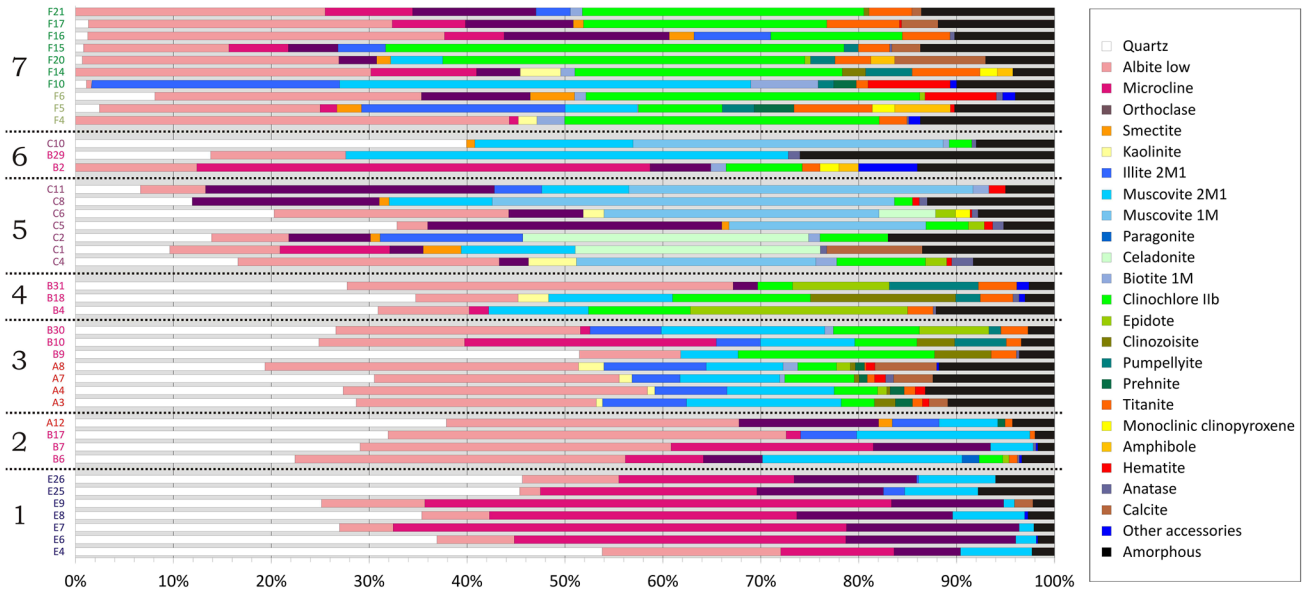

Fig. 8 Quantitative evaluation of the XRPD measurements. Minor phases and varieties occurring in single samples only are merged, but identified structural varieties of micas are indicated. Grouping: 1 – BMR metarhyolites, 2 – SMV (NU) rhyolitic/dacitic rocks, 3 – SMV (NU) andesitic rocks, 4 – SMV (NU) basaltic andesitic rocks, 5 – SMV (SU) metavolcanics, 6 – SMV special rocks (B2 ferroaxinite-containing metavolcanics, B29 pseudotachylite, C10 volcaniclastics), 7 – SMB metabasalts

In consequence of this, pre-deformational textural elements were retained.

Such elements are in some cases recrystallized elliptical objects of a spherulitic lava flow and disharmonically folded flow lamination (Figure B1b). However, such features also can be recognized in other rock bodies of the formation in a more distorted form (Figure B1h), as lava rocks were competent also without silicification. Another, more abundant special texture comprises angular or subrounded lithoclasts or vitroclasts of various sizes up to few centimetres, representing pyroclastics, possibly ignimbrites. Replacement textures are best evidenced on EDX element maps; in Fig. 7c all matrix minerals participate in the substitution of a rounded clast.

Mineralogical and petrographic characteristics of the Szentistvánhegy Metavolcanics

Like chemical, also mineral composition of this formation is heterogeneous. Quartz, albite, potassic feldspars (microcline, orthoclase), dioctahedral mica (phengitic muscovite and illite) and iron-rich clinochlore are the most common rock-forming minerals (Groups 2–4 in Fig. 8). Proportions of these are very variable. Fine-grained matrix is usually coloured in various shades of green by chlorite or of purple by minor amount of additional disseminated hematite. Common accessories are anatase, zircon, fluorapatite and iron oxides.

Phenocrystals of the porphyritic rocks, which rocks are andesitic or dacitic in chemical composition, are angular, idiomorphic, but mostly altered. In rare cases these are still recognizable as relict minerals, like plagioclase and hornblende (Figure B2h, i) or ilmenite (Fig. 7d), but are partly or (in most cases) entirely replaced by fine-grained minerals: albite and potassic feldspars, phyllosilicates, epidote-group minerals, titanite and further accessory minerals like those in the matrix, which are therefore alteration products. Relict zircon and apatite grains are typical for the dacitic and rhyolitic rock samples (Figure B2j). In the andesitic and basaltic rock bodies, primary Ti-(Fe-)oxide minerals (anatase or ilmenite) are added to that (Fig. 7e).

In the NU samples (Groups 2–3 in Fig. 8) dioctahedral micas are of $2M_1$ polytype. Clinochlore was often detected also by XRPD and EPMA to occur as two types, differing mainly in Fe content (Fig. 7e). Further typical minor rock-forming minerals are titanite, epidote-group minerals, and pumpellyite, in some cases also prehnite, concentrated mostly on altered mafic phenocrystals. The amount of these is a few percent mainly in rocks with a low Zr/TiO_2 ratio, where zircon is rare, and chlorite may exceed 10%. In samples of high Zr/TiO_2 ratio clinozoisite and pumpellyite are lacking usually, chlorite and iron-rich epidote are scarce. Titanite often replaces anatase (Figure B2k), with relict patches. Titanite grains show rotation and strain shadows filled by chlorite, and it also appears as overgrowth on distinct grains now completely replaced by chlorite (Fig. 7a). Pumpellyite and epidote-group minerals may appear as fine-grained replacements of plagioclase or mafic minerals, or regular and irregular assemblages in the matrix. Epidote may

reach the tenth millimetres scale, and usually is unoriented, overprinting oriented texture (Figure B2l). It often contains patches enriched in REE (Fig. 7a).

Competent effusive beds of the NU often preserved porphyritic or amygdaloidal textures. The latter ones are basaltic andesites according to their geochemical parameters (relatively low Zr/TiO_2 and high Eu/Eu* values), forming resistant cliffs and ridges in the topography parallel with the strike of the cleavage. Amygdules rarely exceed the millimetre-scale diameter and display various grades of flattening (Figure B2g). Infill can be quartz, calcite and other minerals also present in the matrix.

White or light grey quartz veins like in BMR are common also in this formation, mainly in the Bükkszentlászló block. Large coarse-grained quartz lenses and vein networks, elongated along strike of the cleavage, are embedded in K-Rb-enriched rocks with abundant potassic feldspars and depleted in mafic minerals in their matrix. Appearance and mineral composition of these altered rocks are very similar to the analogous BMR rock type. Less common alterations are represented by sample B1, which is albitized and by sample B2, where relict pyroxene, biotite and metamorphic actinolite, chlorite and titanite typical for basaltic rocks are accompanied by potassic feldspars and axinite (Group 5 in Fig. 8).

The SU samples (Miklós-luga area) are enriched in several cases in K, which is also manifested in an abundance of potassic feldspars and micas, but, in contrast with the NU, these feldspars are mainly orthoclase and not microcline (determined by XRPD), and dioctahedral micas are at least partly of 1M polytype (Group 4 in Fig. 8). Smectites and kaolinite often occur as replacement in pseudomorphs of plagioclase and mafic phenocrystals (Fig. 7f). Biotite (1M) can be found also as retained phenocrystals. Celadonite, chlorite, and epidote represent mafic constituents detected in several samples as replacement mineral bound to individual grains (Figure B2m, n, Fig. 7g). Titanite is lacking here, but anatase was found as a Ti-bearing rock-forming phase (Fig. 7h). Samples of pyroclastics origin retained angular crystalloclasts or vitroclasts, also rounded lithoclasts of some millimetres, occasionally with orientation characteristic for welded rocks (Figure B2c). At some outcrops, both in the Miklós-luga and Bélapátfalva areas, volcanics are mingled with limestone. The increased grain size of the recrystallized calcite at a peperitic contact (Figure B2b) is a signature of hot contact of the lime mud and the volcanogenic material. Sample C10 with a high Zr/TiO_2 ratio, according to its special mineral composition lacking feldspars, might be derived from a redeposited bed.

Amorphous material content is variable according to rock type and mineralogy. The rhyolitic and dacitic rocks of the SMV, similarly to BMR, have developed muscovite and K-feldspars from the original volcanic glass with relatively small residuum. On the other hand, the andesitic and basaltic rocks with more abundant mafic minerals (which are metamorphic or alteration derived) and higher Fe, Mg and Ca concentrations as well have also higher amorphous content, as residual phase in the matrix. The basaltic andesites of the SU have a different mineral composition, often with strong K-metasomatism producing orthoclase and micas. However, their amorphous content is positively correlated with the mafic mineral abundances as well.

Mineralogical and petrographic characteristics of the Szinva Metabasalt

Typical rocks of this formation (excluding peperite) consist of ca. 50% feldspars, mainly albite and a slightly smaller amount of potassic feldspars (microcline and orthoclase) (Group 7 in Fig. 8). Iron-rich clinochlore (IIb polytype) makes another ca. 30% of the rock. Two types of clinochlore differing in Fe content were detected also in several SMB samples just like in SMV. Beyond these, calcite is present in the peperitic rocks, in a variable quantity. Smectite, illite and kaolinite were detected as replacements of altered feldspars. The further rock-forming minerals, which are not always detectable in every sample, are titanite, anatase, hematite, biotite (annite), epidote-group minerals, pumpellyite, prehnite, clinopyroxene and actinolite. Common accessories with quantities below 1% are pyrite (or iron minerals after pyrite), fluorapatite, and zircon.

Clinopyroxene (augite–diopside) occurs as broken, relict phenocrystals partly substituted by amphiboles and smectite (Figure B3a). In some outcrops, albite phenocrystals may also be abundant, showing either intersertal or coarse-grained dolerite texture (Figure B3b, f). However, such bodies usually also have peperitic, bedding-parallel contacts with the host limestone and are, therefore, not intrusive. In some cases, calcite occurs as phenocrystals, nests and possibly vesicle fillings in the texture (Figure B3d). Peperite may form several metres thick beds, usually with cm-scale rounded limestone clasts within a mixed matrix (Figure B3g). Vesicles are recognizable also in non-peperitic rocks of the NU. In the NU samples, in contrast with the fringes typical in CU, chlorite rims (either of vesicles or of clasts) are usually radially oriented (Figure B3h).

Hematite, phengitic muscovite or illite, quartz and rutile abundance are increased in rocks with K-Rb enrichment. Phengite may reach some tens of percent in the composition at the expense of feldspars, which may be completely absent (sample F10). The texture of this rock type is strongly oriented with shear markers and a phyllitic foliation (Figure B3c, e), in contrast with the feldspar-rich varieties. Such rocks, together with some lithoclastic peperite varieties, possibly represent redeposited volcanoclastic material.

The amount of the amorphous material is similar to andesites and basaltic andesites of the SMV and is also related to mafic components, but the interpretation is hindered by the abundance of chlorite. A negative correlation is visible with the proportion of prehnite, pumpellyite and hematite, suggesting that it is the residuum of metamorphic crystallization of volcanic glass. Occurrence of orthoclase, on the other hand, indicates hydrothermal influences.

Discussion

Possible stages of post-magmatic evolution reflected by geochemistry and mineralogy

Compositional variations within the formations may reflect original magmatic differences, post-volcanic alterations, regional metamorphism, and subsequent local metasomatic effects as well. According to our observations, idiomorphic, deformed or fragmented phenocrysts of clinopyroxene, biotite, hornblende, quartz, Fe-Ti oxide minerals, fluorapatite and zircon can be considered as relict minerals of magmatic origin, also altered to various degrees, while further phases (e.g., quartz, feldspars, micas, chlorite in replacement positions or in the fine-grained matrix) are metamorphic or other alteration products. Common secondary features of the metavolcanics within each structural unit can be attributed to regional metamorphism in general. Rock-forming minerals and chemical composition of rock types, which are similar in the geochemical parameters indicating the magmatic origin but are located in different structural units, can be compared to detect local differences in this regional metamorphism. On the other hand, overprinting relationships of the regional and local attributes can help detect the pre-and post-metamorphic alterations.

Local alterations

Common tendencies in the mineral composition of K-enriched and Na-Ca-depleted rocks in each formation indicate a metasomatic alteration affecting both mafic and felsic rocks in all structural units. The consequence is the abundance of potassic feldspars, loss of mafic minerals and depletion of elements hosted by these, and crystallization of hematite. Occasionally, it was also coupled with silicification and formation of quartz veins, most prominently in the Bükkszentlászló block, both in BMR and SMV. As silicified bodies behaved as competent blocks during the development of cleavage and other ductile deformation features, this metasomatism had to precede the regional metamorphism and the synmetamorphic deformation, being possibly a post-volcanic process.

In the case of the BMR most samples plot in the trachyte or trachyandesite fields in Fig. 2, while low trace element concentrations are unusual for such rocks. However, the mineral composition is quite simple, with abundant quartz and hardly any mafic minerals corresponding to a rock of rhyolitic origin. The HFSE depletion found in all sampled rocks of the formation with the same pattern in Fig. 4 can be attributed either to magmatic differentiation or to a subsequent hydrothermal leaching and alteration. It is possible that in the course of the differentiation process, as described by Miller and Mittlefehldt (1982) from other felsic volcanics, the accessories monazite, allanite and zircon were hosting a major part of the REE, while Eu^{2+} was included in plagioclase also, all of which were sorted out by fractional crystallization. On the other hand, variability of the Nb/Y ratio suggests that this situation comes from different grades of depletion of Nb and Y in the samples. Secondary mobility of Nb in the formation is indicated by Nb-oxide minerals formed in quartz-albite veins overprinting the cleavage (Gál et al. 2022). REE tetrad effects in Tetrad 3 only also hint to secondary REE mobility. In that case, the complete formation was metasomatized starting from an original rhyolitic composition, but this process did not affect the now adjacent SMV rocks. Therefore, application of the name metarhyolite can be justified in both cases.

Further specific geochemical and mineral compositions belong to local alteration types overprinting ductile deformation features. These alterations may change the trace element composition including HFSE significantly. HFSE-K enrichment (Németh et al. 2016) was not sampled and studied here. Development of pseudotachylite and albitization

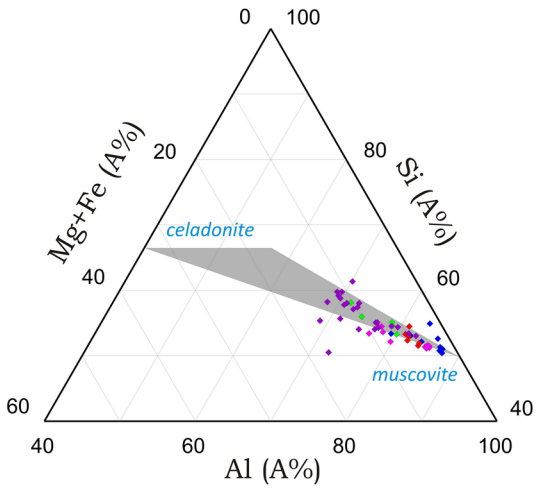

Fig. 9 Mg and Fe substitution measured by EDS results in the sericite matrix of various samples (A3, A4, B1, B18, B30, C1, C5, E6, E25, F14). Colour codes for the plotted data: the same as in Fig. 2

with depletion of K were also observed in some cases, restricted to narrow zones (shear zones and veins, respectively), which are associated with special secondary minerals mostly (Fehér 2015; Gál et al. 2022).

Regional metamorphism and metasomatism

Mineral parageneses in the mafic metavolcanics are typical either for post-magmatic metasomatism (propylitic or spilitic alteration) or for low-grade regional metamorphism. Felsic rocks, on the other hand, do not contain minerals indicative for the metamorphism. This problem was pointed out by Árkai (1973) already, who studied samples from the Szentistvánhegy horizon (SMV), the Bükkszentlászló block (BMR and SMV) and the Lillafüred–Bükkszentkereszt group (SMB). Illite crystallinity (IC) measurements from various metasedimentary and metavolcanic rocks of the Bükk Mts. indicated that the degree of metamorphism is not uniform (Árkai 1983).

Although Árkai (1973, 1983) and Szoldán (1990) mention Ca-rich plagioclase among the rock-forming minerals, in this study exclusively albite and potassic feldspars were eventually identified by XRPD and EPMA in all samples, both as altered phenocrysts, and as matrix components with Plagioclase remnants with higher Ca content were rarely detected in altered grains only. Another major difference is the abundance of titanite, a common phase in all mafic metavolcanics of the NU and CU, exceeding the quantity of epidote-group minerals in the SMB samples, but lacking from samples of SU. A newly observed petrogenetic feature is the phengitic composition of dioctahedral micas, observed in detail by EPMA, with a tendency of higher Mg, Fe, Si and lower Al contents in the less differentiated rock types (Fig. 9). This feature can be a consequence of a generally low Al saturation of the metavolcanics.

Our results show characteristic mineralogical variations corresponding to each structural unit. The relatively highest grade of metamorphism is indicated by the partial transformation of clinopyroxene to actinolite, observed in the SMB samples from the CU, together with formation of clinochlore, pumpellyite, clinozoisite, epidote and titanite. This assemblage corresponds to the pumpellyite–actinolite facies, as Árkai (1983) stated before.

The same assemblage, mostly without clinopyroxene and actinolite, was also observed in the mafic metavolcanics of the NU, both SMV (Bükkszentlászló block) and SMB (samples F1-F4). Prehnite, on the other hand, was detected in few samples only. Despite this, the formation of this assemblage corresponds to the conditions characterizing the prehnite–pumpellyite facies. IC values lower than 0.25 (Árkai 1983) were obtained from the NU and CU, but later 0.25–0.3 was published (Koroknai et al. 2008) from a shear zone at Lillafüred (SMV of the Szentistvánhegy horizon, NU). These IC values also correspond to the observed facies.

Unfortunately, no IC measurements were published from the SU. The coexistence of $2M_1$, 1M muscovite (or illite) and celadonite in the Miklós-luga area (SU SMV), and the lack of titanite and the preserved syngenetic textural elements even in phyllosilicate-dominated rock types indicate that these rocks were altered in a lower p–T regime than those of the NU and CU. The occurrence of muscovite 1M and celadonite restricted to these rock types, together with strong phengitization suggests hydrothermal alteration of volcanic glass. Even if a sharp limit between illite and muscovite cannot be traced, XRD peak sharpness is indicative for the latter. Zeolites, on the other hand, were not detected in any of the samples. The paragenesis of the Miklós-luga

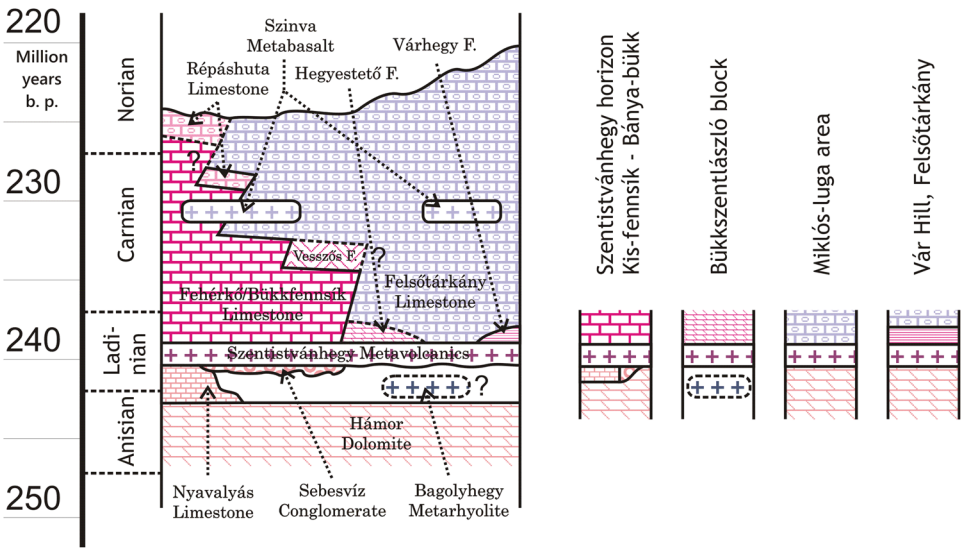

Fig. 10 Probable stratigraphic position of the metavolcanics and adjacent metasedimentary formations in the Middle-Upper Triassic Paraautochthonous successions of the Bükk Mts

area metavolcanics can be compared to the Szarvaskő unit, where a similar mineral composition was interpreted by Árkai (1983) as formed by ocean-floor metamorphism. On the other hand, Ca depletion, relative Na and K enrichment, albitization and replacement of the relict feldspars observed in the SMV samples both of the NU and SU indicate that the same metasomatic stage preceded the progression of the low-grade regional metamorphism in the NU, and this can be applied in the case of SMB as well.

Stratigraphic position of the metavolcanics within the Paraautochthonous unit

The trace element-based identification of the formations in the sampled bodies combined with the mapping of their contacts revealed the stratigraphic relationships shown in Fig. 10. BMR was found in blocks with tectonic contacts exclusively, so its position remains hypothetic. According to zircon U–Pb dating results (~ 247 Ma, but it was measured on metamict zircons with a large proportion of significantly higher ages, Gál et al. 2018), this formation should be older than SMV. SMV zircon U–Pb dating resulted 240 Ma, obtained from samples of the Bükkszentlászló block and of the Szentistvánhegy horizon (Gál et al. 2018). SMV bodies are overlain by various sedimentary formations, ranging from lacustrine to basin facies. According to scarce Ladinian age data (obtained from the Várhegy Formation and from Bükkfensík Limestone, Less et al. 2005), these can be assumed to be coeval, reflecting the heterogeneous topography of the sedimentation area. SMB bodies, probably representing a single horizon, are hosted both by platform and basin facies sediments, from which the Felsőtárkány Limestone was dated to Carnian (Less et al. 2005). Detailed description of the situation is given in Appendix A.

Regional setting of the magmatism

Triassic magmatic formations are not typical in the Western Carpathians (Cros and Szabó 1984; Hovorka and Spišiak 1988; Harangi et al. 1996), but widespread in the Southern Alps and the Dinarides, including the "Pietra Verde" intercalations in sedimentary formations. Metavolcanics (like successfully correlated sedimentary formations, Balogh 1964; Kovács et al. 2000) of the Paraautochthonous Unit were compared to Southern Alpine formations (Cros and Szabó 1984), but without providing trace element geochemistry or radiometric dating, this was based on ambiguous stratigraphic position and incomplete petrographic characterization only.

Triassic successions with outcrops geographically closer to the present-day Bükk Mts. were derived from different terranes (Kovács et al. 2000). The non-metamorphic Transdanubian Triassic succession contains volcaniclastics, lava

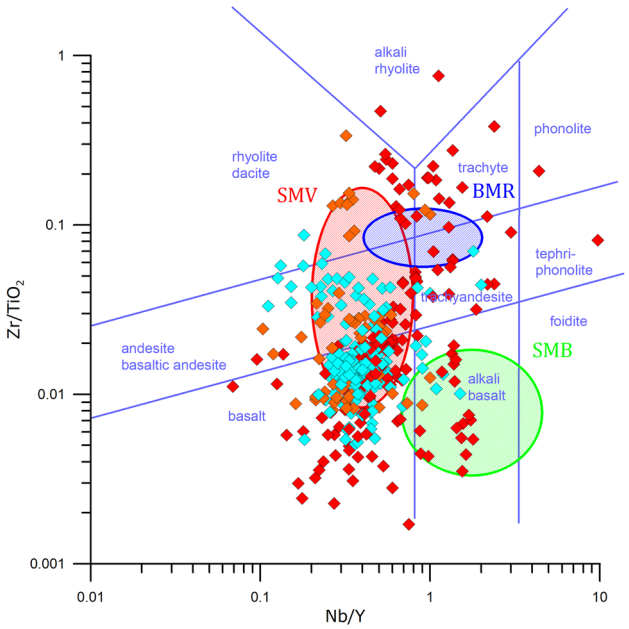

Fig. 11 Classification diagram of Winchester and Floyd (1977) showing ratios calculated from 390 published data of Triassic igneous rock samples from the Southern Alps–Dinarides region, collected by Lustrino et al. (2019). Ellipses indicate the fields of the Bükkian samples from Fig. 2. Fields redefined by Pearce (1996) are shown in blue lines. Colour codes for the plotted data points, according to the classification of Lustrino et al. (2019): cyan – metavolcanics, red – intrusive rocks, orange – unidentified rock type

flows and dikes which were dated to the same Ladinian level as the SMV (Dunkl et al. 2019), but large volcanic complexes and further levels are missing there. The Silica Unit (NW from Bükk Mts) contains Lower Triassic K-rich metarhyolite bodies (Uher et al. 2002) potentially comparable to BMR, but the trace element composition differs completely. Redeposited clasts or olistoliths of the Szarvaskő Unit and the Jurassic mélange formation of the Darnó Zone (Kövér et al. 2018 and sample G2 of this study) can be also excluded from being originated from the Paraautochthonous succession. According to this, comparison should be aimed to the Dinarides and Southern Alps area containing correlated sedimentary and voluminous magmatic formations.

Rocks of igneous origin of the Dinarides are either calc-alkaline suites associated with carbonate platforms of the Outer Dinarides or basalts in nappes of oceanic origin (Pamić 1984). The latter ones can be analogies of the Szarvaskő Unit (Less et al. 2005). The former group has a wide range of rock types but is dominated by basalts; the age constraints are wide as well within Triassic. Most of the rock bodies were described as altered magmatics, spilites and keratophyres (Pamić 1974, 1984).

Reliable radiometric ages are provided from the Southern Alps, where the volcanics are manifold as well. The Triassic magmatics here were described in three groups by Storck

et al. (2019): a Late Anisian–Early Ladinian group dominated by acidic pyroclastics (ignimbrites, redeposited clastics) and additional volcanic stocks; a Late Ladinian group of basaltic (shoshonitic, high-K alkaline) and subordinated trachytic lavas and intrusions, and an Early Carnian group of carbonate-hosted magmatics. The first two groups were dated by zircon U–Pb in the range of 242.7–237.7 Ma; in youngest basalts of the second group, however, there were no zircons to be used for dating. Dating of Late Triassic alkaline basalt dykes of the area were given by Cassinis et al. (2008) based on amphibole $^{40}Ar/^{39}Ar$ dating to ~ 217 Ma, so the magmatism should have lasted up to the Norian stage.

Obenholzner and Pfeiffer (1991) summarized geochemical data of the "Pietra Verde" formations, including Zr/TiO_2 and Nb/Y ratios. Although tuffite samples display a wide scatter, typical values for SiO_2-rich (rhyolitic-dacitic) rocks overlap with the BMR, while those for basaltic rocks are similar to the SMB values. Lustrino et al. (2019) collected published geochemical data of Triassic igneous rocks of the Southern Alps and Dinarides region. In the case of 390 samples Zr, TiO_2, Nb and Y concentrations were all analysed, so these could be plotted in Fig. 11, the same diagram as used for the Bükk samples (Fig. 2). The samples denoted as intrusives show a much wider range of both ratios than those of volcanic origin. Most data points representing metavolcanics are concentrated within the area of the SMV samples, with a dominance of basaltic rocks, while the other two formations, BMR and SMB, correspond mostly to data of intrusive rocks. Volcanic equivalents of these formations seem to be lacking from the dataset. Scatter of the data points, however, reaches far beyond our Bükkian samples.

According to these characteristics and similarly to the palaeontological correlations of the sedimentary rocks, the Triassic metavolcanics of the Bükk Mts. can be compared to the volcanic levels of the Southern Alps and Dinarides, with a marked difference that there are no major intrusive bodies in the Paraautochthonous sequences of the Bükk Mts. The SMV represents the Ladinian volcanic horizon which is the most voluminous both here and in the Southern Alps and Dinarides, although characterized by a higher degree of differentiation in the NU. The other two formations of the Paraautochthonous Unit are not typical in the Alps, but SMB can be the volcanic equivalent of intrusive bodies in the Alps. BMR may represent the proximal formation of an eruptive centre producing the pyroclastic material of the SiO_2-rich "Pietra Verde" beds, although such horizons were not described from the sedimentary formations of the Bükk. In that case, BMR is an initial product, and SMB was formed in late stages of the volcanic evolution of this Tethyan region. However, relation of the BMR to Permian felsic volcanics also occurring in the South Alpine region cannot be excluded as well.

Conclusions

Metavolcanics of the Paraautochthonous successions of the Bükk Mts. can be effectively identified and separated into 3 formations by using the Zr/TiO_2, Nb/Y and Nb/Ta ratios reflecting original composition of the magmatic rocks (Table 3, Figs. 2 and 3). These parameters also can be applied in the case of altered rocks, or rocks containing volcanic material mixed with sediments. Despite this, consideration of further geological, geochemical, and mineralogical observations cannot be avoided, because concentrations of the applied elements and, in consequence, values of these parameters may have been modified by local alterations in some rock bodies.

(1) Bagolyhegy Metarhyolite is a local and unique formation in the Northeastern Unit. It comprises highly differentiated, felsic volcanics of within-plate character. Probably these represent proximal products of a single volcanic centre. The mineral composition is dominated by quartz, albite and potassic feldspars, and dioctahedral micas. Quartz and orthoclase phenocrysts are relict magmatic minerals, while others are metamorphic. Mafic and other accessory minerals are scarce. The chemical composition is characterized by depletion of high field strength elements. Its age and stratigraphic position are uncertain, possibly underlying the Szentistvánhegy Metavolcanics.
(2) Szentistvánhegy Metavolcanics represents a heterogeneous, calc-alkaline volcanic suite with voluminous rock bodies, possibly originated from a chain of several volcanic centres. The volcanism interrupted Ladinian carbonate-dominated marine sedimentation in a wide environment of heterotopic facies. Characteristic rock-forming minerals are quartz, albite, potassic feldspars, phengitic dioctahedral mica, chlorite, titanite and epidote-group minerals. The rock-forming phases are metamorphic, but abundances reflect the original composition.
(3) Szinva Metabasalt represents local submarine alkali basalt flows in Carnian carbonate platforms and basins, mingled with the lime mud. Lava flows and adjacent volcaniclastics may reach the thickness of some ten metres and lateral extents of some kilometres. Rock-forming minerals are relict magmatic clinopyroxene and metamorphic albite, potassic feldspars, chlorite, titanite and epidote-group minerals. A significant part of the rocks is peperite with calcite as additional rock-forming mineral. Geochemical composition indicates within-plate character.

Local characteristics of the metavolcanics depend partly on composition of the magma and on metasomatic alterations affecting the rocks unevenly. Such alterations originated before and after regional metamorphism of the rocks.

Differences in metamorphic facies bound to structural units were also observed. Occurrence of mineral assemblages and indicator minerals in mafic rock types of the Szentistvánhegy Metavolcanics and the Szinva Metabasalt can be used for comparison. Metamorphism reached the pumpellyite–actinolite facies in the Szinva Metabasalt of the Central Unit, and pumpellyite–prehnite facies in the Northeastern Unit. In the Szentistvánhegy Metavolcanics of the Southeastern Unit ocean-floor-type metasomatism is indicated, which may have preceded the progression of low-grade regional metamorphism also in the Northeastern Unit. The tectofacies-based separation is supported by the differences in metamorphic facies.

Supplementary Information The online version contains supplementary material available at https://doi.org/10.1007/s00531-022-02246-6.

Acknowledgements The authors thank the colleagues at the University of Miskolc (D. Debus, M. Leskó, R. Papp and N. Zajzon) for their support in sample preparation and laboratory tests, and for the reviewers (especially for I. Broska) for their constructive remarks and support in improving the article.

Funding Open access funding provided by University of Miskolc. The research was carried out at the University of Miskolc both as part of the project implemented in the framework of the Thematic Excellence Program funded by the Ministry of Innovation and Technology of Hungary, and the project supported by the Ministry of Innovation and Technology of Hungary from the National Research, Development and Innovation Fund in line with the Grant Contract (reg. nr.: NKFIH-846-8/2019) issued by the National Research, Development and Innovation Office. The work of P. Gál was supported by the ÚNKP-19-3 New National Excellence Program of the Ministry for Innovation and Technology.

References

Árkai P (1973) Pumpellyite-prehnite-quartz facies Alpine metamorphism in the middle Triassic volcanogenic-sedimentary sequences of the Bükk mountains, NE Hungary. Acta Geol Hung 17(1–3):67–83

Árkai P (1983) Very low- and low-grade Alpine regional metamorphism of the Paleozoic and Mesozoic formations of the Bükkium, NE-Hungary. Acta Geol Hung 26(1–2):83–101

Árkai P, Balogh K, Dunkl I (1995) Timing of low temperature metamorphism and cooling of the Paleozoic and Mesozoic formations of the Bükkium, innermost western Carpathians, Hungary. Geol Rundsch 84(2):334–344

Balla Z (1983) Succession and tectonics of the Szarvaskő Synform. Annual report of the MÁELGI from 1982, pp 42–65 (in Hungarian)

Balogh K (1964) Geological formations of the Bükk Mts. MÁFI yearbook 48/2: 245–553 (in Hungarian and in German) http://epa.oszk.hu/03200/03274/00101/pdf/

Cassinis G, Cortesogno L, Gaggero L, Perotti CR, Buzzi L (2008) Permian to Triassic geodynamic and magmatic evolution of the Brescian Prealps (eastern Lombardy, Italy). Ital J Geosci 127(3):501–518

Cros P, Szabó I (1984) Comparison of the Triassic volcanogenic formations in Hungary and in the Alps. Acta Geol Hung 27(3–4):265–276

Csontos L (1999) Structural outline of the Bükk Mts (N Hungary). Földtani Közlöny 129(4):611–651 (**in Hungarian**)

Dobosi G (1986) Clinopyroxene composition of some Mesozoic igneous rocks of Hungary: the possibility of identification of their magma type and tectonic setting. Ofioliti (Italy) 11(1):19–34

Dunkl I, Farics É, Józsa S, Lukács R, Haas J, Budai T (2019) Traces of Carnian volcanic activity in the Transdanubian range, Hungary. Int J Earth Sci 108:1451–1466. https://doi.org/10.1007/s00531-019-01714-w

Fehér B (2015) Hydrothermal breccia with tourmaline cement from Miskolc-Bükkszentlászló. Herman Ottó Museum Yearbook 54:11–23 (**in Hungarian**)

Gál P, Németh N, Szakáll S, Zajzon N, Fehér B, Dunkl I (2022) Nb-Ta mineralization in Ti-oxide minerals from the Bagolyhegy Metarhyolite Formation (Bükk Mountains, NE Hungary). Central Eur Geol 65:1–13. https://doi.org/10.1556/24.2021.00101

Gál P, Lukács R, Józsa S, Dunkl I, Németh N, Harangi Sz (2018) Results of the petrographical, geochemical and geochronological reinvestigation of the Triassic metavolcanic rocks at Bükkszentlászló, Bükk Mts. (NE Hungary). Geologica Balcanica, XXI International Congress of the Carpathian Balkan, Geological Association (CBGA), Abstracts, p. 125. https://www.geologica-balcanica.eu/sites/default/files/default/files/abstract-books/Geol_Balc_CBGA_2018%20%28eBook%29.pdf

Harangi Sz, Szabó Cs, Józsa S, Szoldán Zs, Árva-Sós E, Balla M, Kubovics I (1996) Mesozoic igneous suites in Hungary: implications for genesis and tectonic setting in the northwestern part of Tethys. Int Geol Rev 38:336–360

Hovorka D, Spišiak J (1988) Mesozoic volcanism of the Western Carpathians. Veda, Bratislava (**in Slovakian with English summary**)

Kiss G, Molnár F, Kovács S, Palinkaš LA (2010) Field characteristics and petrography of the advanced rifting related Triassic submarine basaltic blocks in the Jurassic mélange of the Darnó Unit. Central Eur Geol 53(2–3):181–204

Kiss GB, Molnár F, Palinkaš LA (2016) Hydrothermal processes related to some Triassic and Jurassic submarine basaltic complexes in Northeastern Hungary, the Dinarides and Hellenides. Geol Croatica 69(1):39–64

Koroknai B, Árkai P, Horváth P, Balogh K (2008) Anatomy of a transitional brittle–ductile shear zone developed in a low-T metaandesite tuff: a microstructural, petrological and geochronological case study from the Bükk Mts (NE Hungary). J Struct Geol 30(2):159–176

Kovács S, Haas J, Császár G, Szederkényi T, Buda Gy, Nagymarosy A (2000) Tectonostratigraphic terranes in the pre-Neogene basement

of the Hungarian part of the Pannonian area. Acta Geol Hung 43(3):225–328
Kövér S, Fodor L, Kovács Z, Klötzli U, Haas J, Zajzon N, Szabó Cs (2018) Late Triassic acidic volcanic clasts in different Neotethyan sedimentary mélanges: paleogeographic and geodynamic implications. Int J Earth Sci 107:2975–2998. https://doi.org/10.1007/s00531-018-1638-2
Kubovics I, Nagy B, Nagy B-né, Puskás Z (1989) Beryllium and some other rare element contents of acid volcanics (tuffs) and metamorphites in Hungary. Acta Geol Hung 21:219–231
Less Gy, Kovács S, Pelikán P, Pentelényi L, Sásdi L (2005) Geology of the Bükk Mts. Explanatory book to the geological map of the Bükk Mountains (1: 50000). Geological Institute of Hungary, Budapest (**in Hungarian**). https://mbfsz.gov.hu/sites/default/files/file/2018/03/23/bukk_magy_egesz.pdf
Lustrino M, Abbas H, Agostini S, Caggiatie M, Carminati E, Gianolla P (2019) Origin of Triassic magmatism of the Southern Alps (Italy): constraints from geochemistry and Sr-Nd-Pb isotopic ratios. Gondwana Res 75:218–238. https://doi.org/10.1016/j.gr.2019.04.011
McDonough WF, Sun SS (1995) The composition of the earth. Chem Geol 120:223–253
Mezősi J (1950) Rock provincial setting of the Bükk Mts. of Borsod County. Acta Universitatis Szegediensis Mineralogica, Petrographica 4:50–55 (**in Hungarian**)
Miller CF, Mittlefehldt DW (1982) Depletion of light rare-earth elements in felsic magmas. Geology 10(3):129–133
Monecke T, Kempe U, Monecke J, Sala M, Wolf D (2002) Tetrad effect in rare earth element distribution patterns: a method of quantification with application to rock and mineral samples from granite-related rare metal deposits. Geochim Cosmochim Acta 66(7):1185–1196. https://doi.org/10.1016/S0016-7037(01)00849-3
Németh N, Mádai F (2005) Early phase ductile deformation elements in the limestone of the eastern part of the Bükk Mts. Hungary Acta Geologica Hungarica 48(3):283–297
Németh N, Pethő G, Zajzon N (2015) In situ gamma ray survey for geological mapping of K-metasomatized metavolcanics at Bükkszentkereszt, Bükk Mts, Hungary. Open Geosci 7:318–331. https://doi.org/10.1515/geo-2015-0033
Németh N, Baracza MK, Kristály F, Móricz F, Pethő G, Zajzon N (2016) Rare earth and rare element mineralization in metavolcanic rock bodies in the SE part of the Bükk Mts. Földtani Közlöny 146(1):11–25 (**in Hungarian with English abstract**)
Obenholzner H, Pfeiffer J (1991) "Pietra Verde" – a contribution to the geodynamics of the Southern Alps. Jubiläumsschrift 20 Jahre Geologische Zusammenarbeit Österreich – Ungarn, Teil 1, pp 221–245 (in German)
Ozdín D, Szakáll S (2014) Chemical composition of axinite-(Fe) from Miskolc-Lillafüred, Bükk mountains Hungary. In: Fehér B (ed) In the attraction of minerals. Studies in honour of the 60-year-old Sándor Szakáll. Herman Ottó Museum, Miskolc, pp 203–217
Pamić J (1974) Middle Triassic spilite-keratophyre association of the Dinarides and its position in Alpine magmatic-tectonic cycle. In: Amstutz GC (ed) Spilites and spilitic rocks. IUGS Series A 4, pp 161–174
Pamić J (1984) Triassic magmatism of the Dinarides in Yugoslavia. Tectonophysics 109:273–307
Pantó G (1951) Geology of the southern igneous belt in the eastern part of Bükk Mts. Földtani Közlöny 81:137–145 (**in Hungarian with English abstract**)
Pearce JA (1982) Trace element characteristics of lavas from destructive plate boundaries. In: Thorpe RS (ed) Andesites. John Wiley, Chichester, pp 525–547
Pearce JA (1996) A users guide to basalt discrimination diagrams. In: Wyman DA (ed) Trace element geochemistry of volcanic rocks: applications for massive sulphide exploration. Geological Association of Canada, Short Course Notes 12, pp 79–113
Pelikán P (1999) Triassic and Jurassic formations of the area of borehole Felsőtárkány-7 (Bükk Mts, N Hungary). Földtani Közlöny 129(4):593–609 (**in Hungarian**)
Storck J-C, Brack P, Wotzlaw J-F, Ulmer P (2019) Timing and evolution of Middle Triassic magmatism in the Southern Alps (northern Italy). J Geol Soc 176:253–268
Szabó I, Vincze J (2013) U-Be-bearing and Mn-ore associated phosphate mineralization of the rhyolite (quartzporphyry)-tuff, at Bükkszentkereszt (NE Hungary). Földtani Közlöny 143(1):3–28 (**in Hungarian**)
Szakáll S, Földvári M (1995) New minerals of Hungary III. Ferroaxinite and chrysocolla from Miskolc-Lillafüred (Bükk Mts). Földtani Közlöny 125/3–4:433–442 (in Hungarian with English abstract)
Szakáll S, Kristály F, Zajzon N, Németh N, Fehér B (2012) Secondary phosphates and sulphates in the silicified metarhyolite of the Fényeskő Valley at Diósgyőr. Yearb Herman Ottó Mus 50:35–46 (**in Hungarian**)
Szentpétery Zs (1923) Geological setting of the paleo- and mesoeruptive rocks from the vicinity of Diósgyőr and Szarvaskő. Annual report of the Geological Institute of Hungary from 1917–19, pp 75–88 (**in Hungarian**)
Szentpétery Zs (1929a) Rock types from the vicinity of Lillafüred. Acta Chemica, Mineralogica et Physica 1:10–43 (**in German**)
Szentpétery Zs (1929b) Eruptive suite in the Savós Valley at Lillafüred. Acta Chem Mineral Phys 1:72–128 (**in German**)
Szentpétery Zs (1931) Quartz porphyry of the Bagoly Hill at Lillafüred. Acta Chem Mineral Phys 2(2):81–108 (**in Hungarian**)
Szentpétery Zs (1932) New contributions to the petrology of the Savós Valley at Lillafüred. Acta Chem Mineral Phys 2:24–46 (**in German**)
Szentpétery Zs (1934a) Porphyry suite over Hámor in the Bükk Mts. Acta Chem Mineral Phys 3:149–181 (**in German**)
Szentpétery Zs (1934b) Petrological features of the Fehérkő Hill and description of its eruptive rocks in detail. Acta Chem Mineral Phys 4:18–123 (**in German**)
Szentpétery Zs (1935) Eruptive part of the bottom of Fehérkő Hill at Lillafüred. Matematikai és Természettudományi Értesítő 52:253–286 (**in Hungarian**)
Szentpétery Zs (1936) General petrography of the eruptive rocks of the Szentistván Hill at Lillafüred. Matematikai és Természettudományi Értesítő 54:279–308 (**in Hungarian**)
Szentpétery Zs (1937) Stratovolcanic part of the Szentistván Hill in the Bükk Mts. Acta Chem Mineral Phys 5:26–134 (**in German**)
Szentpétery Zs (1950a) Data to the introduction of the diabase in the Bükk Mts. Földtani Közlöny 80:168–183 (**in Hungarian**)
Szentpétery Zs (1950b) Diabase types of the Lőrinc Hill at Újhuta in the Bükk Mts. Földtani Közlöny 80:316–323 (**in Hungarian**)
Szoldán Zs (1990) Middle Triassic magmatic sequences from different tectonic settings in the Bükk Mts. NE Hungary. Acta Mineral-Petrogr 31:25–42
Tóth ZH, Kristály F (2017) Archaeometrical studies on white Szeletian felsitic porphyry. Archeometriai Műhely 14(2):85–98 (**in Hungarian**)
Uher P, Ondrejka M, Spišiak J, Broska I, Putiš M (2002) Lower Triassic potassium-rich rhyolites of the silicic unit, Western Carpathians, Slovakia: geochemistry, mineralogy and genetic aspects. Geol Carpath 53(1):27–36
Velledits F (1999) Anisian terrestrial deposits in the sequences of the Northern Bükk Mts (Anisian-Ladinian layers of the Alsó-Sebesvíz key section and Miskolc-10 borehole = Zsófiatorony). Földtani Közlöny 129(3):327–361 (**in Hungarian**)

Winchester JA, Floyd PA (1977) Geochemical discrimination of different magma series and their differentiation products using immobile elements. Chem Geol 20:325–343

Zajzon N, Németh N, Szakáll S, Gál P, Kristály F, Móricz F (2014) Rare earth elements in the Mn-U-Be geochemical anomaly at Bükkszentkereszt. In: Szakáll S (ed) Rare earth elements in the geological formations in Hungary. CriticEl Monogaphy Series 5, Milagrossa Kft, Miskolc, pp 91–108 (**in Hungarian**)